Scientific Research Publishing

Open Journal of Geology, 2023, 13, 136-170
https://www.scirp.org/journal/ojg
ISSN Online: 2161-7589
ISSN Print: 2161-7570

Effects on Sedimentary Processes via Upper Triassic Climate Forcing Caused by Multiple Impacting and Large Igneous Provinces (LIP)-Rifting/Degassing: Jordanian Platform/Arabian Plate and Germanic Basin/Central Europe

Werner Schneider[1], Elias Salameh[2]

[1]Formerly Braunschweig Technical University, Braunschweig, Germany
[2]University of Jordan, Amman, Jordan
Email: salameli@ju.edu.jo

How to cite this paper: Schneider, W. and Salameh, E. (2023) Effects on Sedimentary Processes via Upper Triassic Climate Forcing Caused by Multiple Impacting and Large Igneous Provinces (LIP)-Rifting/Degassing: Jordanian Platform/Arabian Plate and Germanic Basin/Central Europe. *Open Journal of Geology*, **13**, 136-170.
https://doi.org/10.4236/ojg.2023.132007

Received: November 25, 2022
Accepted: February 14, 2023
Published: February 17, 2023

Abstract

Upper Triassic sedimentary systems of both the Arabian Plate and the Germanic Basin reveal climate- and plate tectonic-forced effects through certain time-intervals experienced by architectural elements, lithofacies types, unconformities, flash flood deposits, maximum flooding surfaces/sequence boundary (MFS/SB), mineralogy, and isotope anomalies. Further, Moon recession and changes of Earth's rotation velocity (core/mantle boundary) are associated with multiple impacting and large igneous provinces/Mid Oceanic Ridge Basalt, LIP/MORB-rifting/degassing. While acidification (by degassing, sturz-rain) does influence tectosilicates and carbonates, montmorillonite represents a key mineral as transformation of volcanic/impact glass (Tephra) to be found as co-components in and in certain pelite units as "boundary clay-suspicions" (mixture of eolian paleoloess, pelite, paleosol, and tephra ➡ tuffite). Obviously, unconformities and sequence boundaries of both study areas separate and dislocate interrupted $\partial^{13}C$ and $^{87}Sr/^{86}Sr$-data groups along the isotope curves. Both Proto-Arctic Ocean rifting/degassing comprising kimberlitic pyroclastic eruptions and Neotethys rifting/degassing as well as multiple impacting played the most important role during the Norian, followed by the incipient Central Atlantic Magmatic Provinces rifting since the Rhaetian. The following associations are encountered and dealt with in this study: Sequence boundaries-$\partial^{13}C$, maximum flooding surfaces-(FUCs)-$\partial^{13}C$, unconformities-plate motion, tephra-pelite-tuffite-montmorillonite. Norian: maximum flooding surfaces

(MFSs)-"paleosol"/boundary clay?-rifting-volcanism, Moon/Earth data change. So the Norian (~221 - 206 Ma) hosts anomalous "amalgamated maximum flooding surfaces (MFSs)", amalgamated paleosol (Jordanian Platform), multiple impacting (~219 - 214 Ma), the maximum opening of the Proto-Arctic Ocean (PAO) (~230 - 200 Ma), Neo-Tethys (NT)-subvolcanic (sills, dikes) in the NE Dead Sea area prior the Rhaetian, and a significant change of Earth/Moon relation data. The study concludes that rare and extreme events are very strongly shaping the geologic constellations in the Earth System.

Keywords

Endogenic and Impact Drivers, Sedimentary Effects, Interplay Processing, Event-Stratigraphy

1. Introduction

Several Phanerozoic siliciclastic systems (Cambrian, Lower Ordovician, Upper Permian, Lower Cretaceous) deposited on the Jordanian Platform, expose an abrupt change of sedimentologic pattern (*i.e.* architectural elements, lithofacies, mineral assemblage) matching formation boundaries and climate changes [1] [2].

Moreover, they meet plates' track course change (direction, speed) originally interpreted as effect of major impacting [3] (**Table 1**, **Figure 1**).

Meanwhile accepted, magmatic degassing (via rifting, plume, Mid Atlantic Rifting Basalts (MORB), subduction) plays the most dominant role with regard to formation boundaries and mass extinction [4]-[11]. Additionally, heated sedimentary formations (marl, bituminous shale, hydrocarbons, carbonate rocks, evaporates) may even dominantly contribute via volatile release from sill and dike intrusions to climate forcing, metal toxicity and consequently to mass extinction [11] [12]. Besides the common greenhouse, gases, as less known, components of erupted gas methylchloride/methylbromide are seen as main drivers for global warming and ozone depletion, too.

To better understand that degassing induced "indirect effects" on siliciclastics, it is helpful to distinguish positive climate forcing (greenhouse gases, solar radiation)

Table 1. Plates track change during the triassic period [3] Ma.

Plate	PTB				PTB		➡TJB Ma	
Borneo	250	238	230	-	220	208	200	-
Hawai	250	238	230	225	220	208	200	195
Madagaskar	250	-	230	-	220	208	-	195
Mariana	250	238	230	-	220	208	-	195
Japan	250	238	230	225	220	-	-	195
N America	250	238	230	-	220	208	-	195
S America	250	238	230	-	220	208	-	195

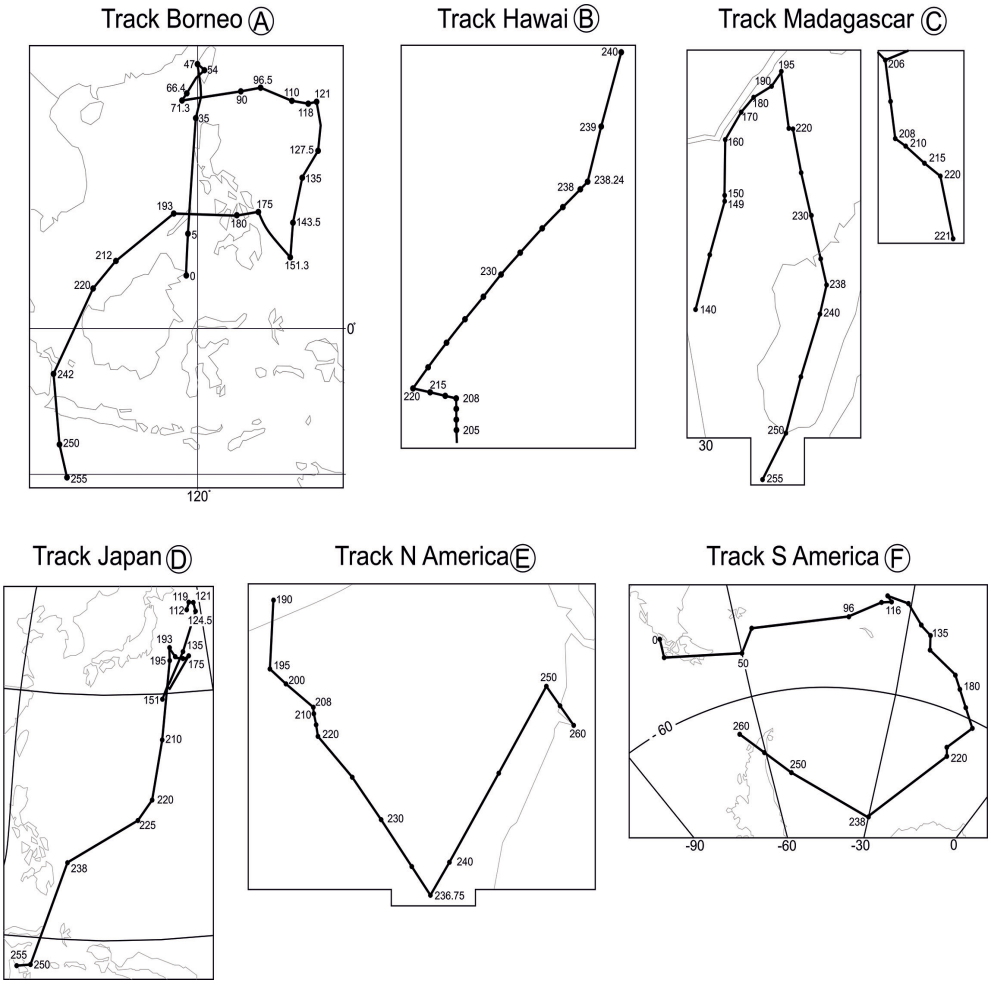

Figure 1. Track change of plates (direction, speed) during the Triassic time-span relating to the markers of A: Hawaii, B: Borneo, C: Madagascar, D: Japan, E: S America, F: N America [3], (**Table 1**).

versus negative climate forcing (tropospheric aerosols, ozone depletion, clouding, acid rain, volcanism, tephra, soot) [13].

Based on long-term fieldwork including mineralogic studies on the Jordanian Platform [1] [2] and the Germanic Basin [14] [15] [16] [17] [18], the Upper Triassic sedimentary sequences of both study areas evidence relations of sedimentologic/petrologic data to indirect effects caused by multiple impacting and LIP-/plate tectonics-generated exhalations [9].

Multiple impacting is represented by the meteorite craters of San Martin /Canada, Obolon/Ukraine, Rochechouart/France, Manicouagan/Canada, and Red Wing/Canada [19] [20] [21] [22] (**Table 2**), while the occurrences of planar deformation structures (PDS) in quartz grains embedded in Upper Rhaetian pelite, Apennine Mts./Italy, indicate possibly a boundary clay [23].

Major degassing occurred during the Neo-Tethys rifting (NT) [24] [25], the Gondwana LIP [8] [9], the Central and Eastern Arctic LIP/Proto-Arctic (Anyui) Ocean (PAO: [7]) and in the Central Atlantic Magmatic Province (CAMP): [9] [26] [27] [28] all of them affected the end-Triassic crisis (**Figure 2**).

Table 2. Multiple impacting and LIP/MORB activity through the Upper.

Event	References	Age (Ma) Method	LIP/MORB (km) crater Ø	Target Rocks [19] [21]
Red Wing USA	[19] [21]	200 ± 25?	9	Carbonates, ⬅ sandstone evaporites
Wells Creak, USA	[19] [21]	200 ± 100?	12	
Nova Scotia (CAMP)	[22] [27]	201.4 ± 1	Rift	
Italy (multiple)	[23]	Up. Rhaetian	PDS	Rhaetian sediments
Proto Arctic Ocean (PAO)	[7]	206 - 200 Rhaetian	Rift	
Triassic/Jurassic B.	[22] [27]	201.4 U/Pb		
Mass Extinction	[62] [63]	Zircon		
Manicouagan, Canada	[19] [21]	214 ± 1 U/Pb, Zircon	100	Metamorphic ⬅ rocks, anorthosite
Rochechouart, France	[19] [21]	214 ± 8 $^{40}Ar/^{39}Ar$	25	Crystalline rocks
Obolon, Ukraine	[19] [21]	215 ± 25?	15	Gneiss, granitoids, sediment cover
San Martin, Canada	[19] [21]	219 ± 32	40	Granite, gneiss, Paleozoic sedim. cover
Mass Extinction	[62] [63]	220 (Carnian/Norian B.)		
Proto Arctic Ocean (PAO)	[7]	230 - 220 (Carnian	Rift	

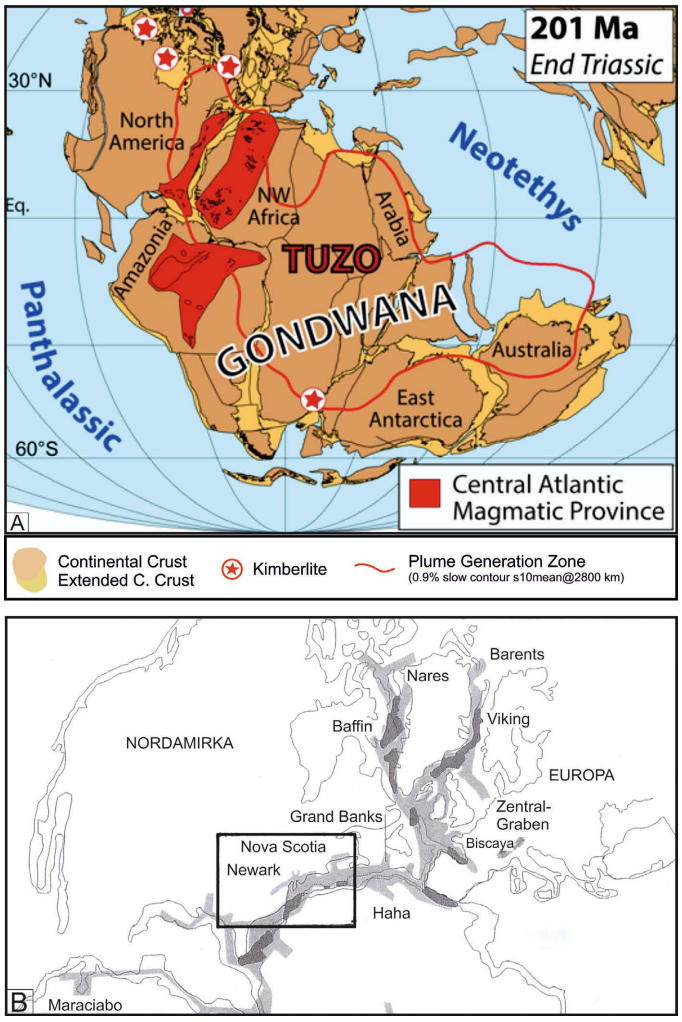

Figure 2. Paleogeography of the Triassic. A: Gondwana and plume generation zone (paleogeographic reconstruction) with the position of Arabia and Jordan. B: Incipient rifting in the N Atlantic, Nova Scotia/ Newark [28].

Price's ATLAS-data [3] (**Figure 1**) exhibit plate motion between 210 and 208 Ma based on the markers at Borneo, Hawaii, Madagascar, Japan, N/S America, s. America and Mariana that interrelate with geodynamic processes (**Table 1**).

Physico-chemical/mineralogical affection by geodynamic processes via hazardous events relating to climate forcing (acidic sturz rain, flash flooding, whirl storm, metal toxicity, ocean acidification, architectural elements, lithofacies, pH, Eh) has been recently experienced by revisiting the Permian-Triassic boundary (PTB) [29] and the Cretaceous-Tertiary boundary (KPgB) [30].

The study tries to clarify the Norian anomalous "amalgamated" maximum flooding surfaces, the amalgamated paleosol on the Jordanian Platform, the multiple impacting, the maximum opening of the Proto-Arctic Ocean, Neo-Tethys (NT)-sub-volcanic sills and dikes in the NE Dead Sea area prior the Rhaetian, and the significant change of Earth/Moon relation data.

2. Methodology

In this article different published and unpublished works of the authors and other workers in the Germanic Basin and in Jordan have been interpreted and correlated with triggering rare events such as volcanic eruptions, meteoritic impacts, tsunamis, maximum flooding etc. Most of the basic data stems from original work of the authors associated with other published works.

The idea and the interpretation of correlating former geologic findings to rare and extreme events is the sole work of the authors.

3. Jordanian Platform/Arabian Plate

As part of N Gondwana, the Arabian Plate fronted the newly opened Neotethys (NT) along a passive margin since the Permian [8] [24] [25]. Its shelf areas (Saudi Arabia, Oman) expose sedimentary cycles of eight recurrent Maximum Flooding Surfaces (MFSs) Tr 10 to Tr 80 with time intervals of ~6 to 9 Ma (**Figure 3**).

A kind of "MFS-amalgamation" (Tr 70a,b,c: ~220 to 211 Ma) originated asymmetrically: a fast developing Transgressive System Track (TST) up to the Maximum Flooding Surface (MFS) was followed by a Regressive System Track (RST) revealing sabkha facies (dolomite, sulfate), finally overlain with clastics towards a Low Stand System Track (LST, SB) (**Figure 3A**). The lateral extension of the MFSs decreases northwestward (Jordanian Platform) [25].

This sequence meets the time-span of the impact events of San Martin (219 ± 32 Ma), Rochechouart (214 ± 8 Ma), Obolon (215 ± 25) and Manicouagan (214 ± 1 Ma), [19] [20] [21] [22] (**Table 2**).

On the Jordanian Platform, where the NT-transgression southward continued through the Triassic, intertidal and shallow subtidal environments cyclically alternated, intercalated by a few off-shore or a supertidal excursion [31] [32] [33] (**Figure 3**), all in all documenting a labile balance of subsidence and sedimentation rate in front of the stable hinterland from where siliciclastic input occasionally continued.

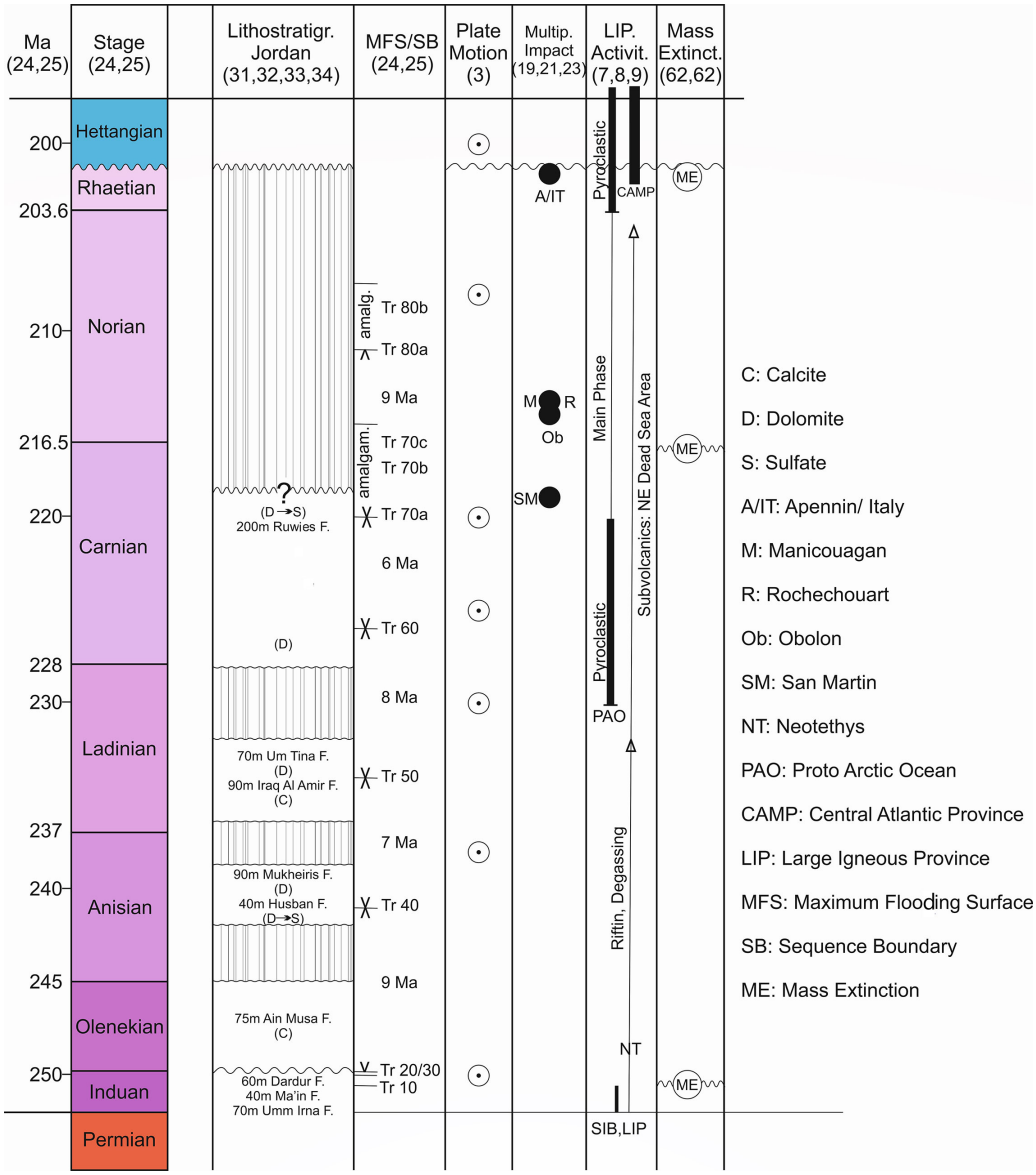

Figure 3. Chart of the Jordanian Platform for the Triassic, exposing intertidal/subtidal cycles intercalated by unconformities relating to MFSs/SBs on the Arabian shelf (Saudi Arabia, Oman). The cyclic limestone/dolomite occurrences mirror temperature change. A ~8 m thick "amalgamated" paleosol originated since the Carnian up to the TJB. Note coincidences with plate motion, multiple impacting and LIP activities.

While the Lower Triassic siliciclastic yield alternatingly calcite/dolomite cement (Ma'in F. to Iraq Al Amir F.), the upper portion (Um Tina F. to Ruweis F.) own dolomite/sulfate cement indicating an increasing Mg/Ca-ratio of vadose brine during increasing aridity through the SB-interval [31] [32] [33].

A correlation of both Platform and Shelf deposits appears hard without $\partial^{13}C$-data. An exception may be given by the euryhaline foraminifera-bearing limestone near the base of the Nimra M./Lower Scythian, possibly correlating with the MFS Tr 10 [25] [31] [33]. The Dardur F./Upper Scythian bears conodonts while Anisian ammonites are found in the Hisban F./Anisian.

The Iraq Al Amir/Tina F. boundary may be approximately set around the Ladinian/Carnian boundary; the Ruweis F. presents a Carnian age [31] [32] [33]. Its lower portion exposes cyclic dolomite/sulfate deposits, atop plant fragments and leached evaporates. The upper portion built up with alternating laminated dolomite, anhydrite and shale, exhibits widespread sabkhas, saline pools and intertidal environments. MFS Tr 60 [25] and a track change (**Figure 1**), Japan [3] coincide with plate motion around ~225 Ma.

With the beginning of multiple impacting (Tr 70: ~220 Ma) by the San Martin event [18], the lower portion of the Carnian Ruweis F. became overlain with an 8 m thick "amalgamated paleosol" (**Figure 4A**, **Figure 4B** [34]) subdivided by four main Units (1-4) each separated from the next one by limonite/hematite encrustations of pedogenetic origin under arid climate.

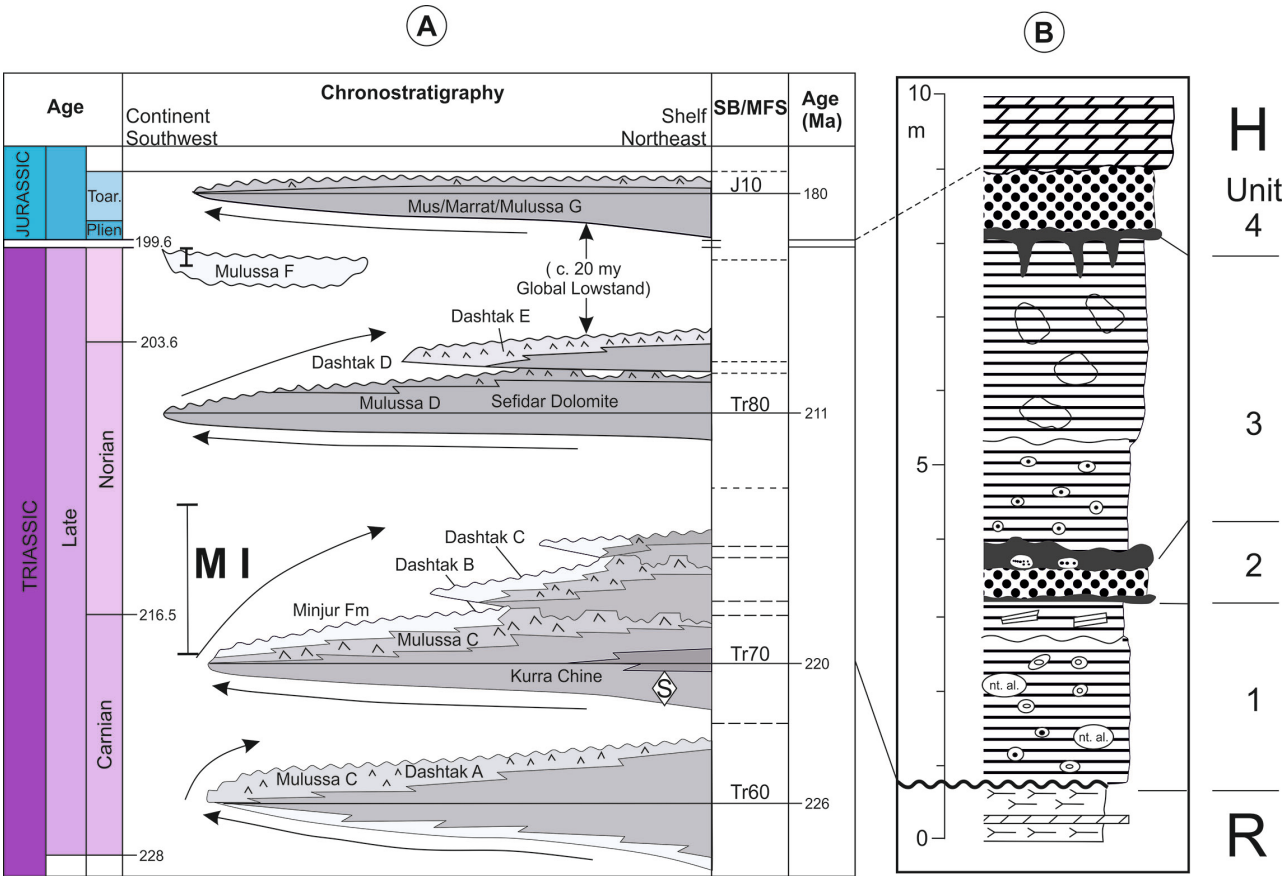

Figure 4. The paleosol formation on the Jordanian Platform coincides with two "amalgamated" MFSs (Tr 70a,b,c, Tr 80a,b) on the Arabian Shelf (A). The first one meets multiple impacting (MI) while both relate to LIP-activities. The polygenetic paleosol (B) overlies the evaporatic Ruweis F. and comprises four units: Unit 1: Massive structureless red-braun claystone bearing ferrogenous glaebules and patches of natroalunite; the upper portion contains coalified and limonitized wood fragments (boundary clay-suspicious?). Unit 2: Yellowish colored friable sandstone, at the base and top Fe-encrustations. Unit 3: Irregular limonite encrustation of violet/dark red color at base overlain with massive structureless red claystone bearing Fe-glaebules and resembling Unit 1. XRD analysis reveals kaolinite, illite, irregular illite/smectite mixed layer and a kaolinite/sudoite mixed layer, enrichment of Ba (1136 ppm) and B (817 ppm), [33]. Unit 4: At base dessication cracks filled with Fe-encrustations, overlain with yellowish-colored friable sandstone (comp. Unit 2), kaolinite and natroalunite-bearing shards of quartz grains are strongly corroded (comp. PTB [29]). Jurassic carbonate rocks overlie the complex paleosol above the unconformity.

Of special interest are two structure-less grey-violet pelite layers (Units 1 and 3) bearing Fe-glaebules and natroalunite in a kaolinitic matrix whose upper portions contain coalified/limonitized wood fragments. Both Units' clay mineral assemblage reveal besides kaolinite, illite, illite-smectite and kaolinite sudoite irregular mixed layers, while the Fe-encrustation yields high corroded shards of quartz grains indicating temperature/pH-shock ([34] comp. [29]). The well-sorted siliciclastic intercalations structure-less, too, may be of "eolian" origin. The Units 1 and 3 appear as "boundary clay suspicious" to be discussed below.

The uppermost part of the "paleosol-complex" and the hiatus to the Lower Jurassic meets the time-span of the Newark Supergroup volcanics, New Scotia/Central Atlantic Magmatic Province (CAMP), (~220 - 201 Ma): [19] [21] [22] [27] and the eruption of kimberlitic pyroclastics during maximum opening of the Primary Arctic Ocean (PAO) over large parts of the Siberian Craton [7]; (**Figure 3**).

Furthermore, apart from the Upper Triassic Impact events and LIPs (CAMP, PAO), subvolcanic sills and dikes intruded along the NE Dead Sea area into the Cambrian and Triassic sequences without having passed the Triassic/Jurassic boundary (TJB ~20 Ma), [35].

Their pertrologic spectrum comprises alkaline-gabbro, trachyte and trachyte-andesite of strong alkaline character to be derived from continental rift magmatism as part of the Mesozoic igneous activity that affected Jordan and adjacent areas corresponding to the Neo-Tethys-rifting to generate the passive continental margin of the Levant Basin/Eastern Mediterranean and provided part of the degassing scenery throughout the Upper Triassic, including the Asher volcanism in N-Palestine [36].

4. Germanic Basin/Central European Basin

The epicontinental Germanic Basin was formed after the Variscan Mts. Building. It belongs to the northern branch of the peri-Tethyan Basin modified by regional synsedimentary and salt tectonics [14] [37] [38] (**Figures 5A-F**).

Surrounded by the source areas of the Fennoscandic-Baltic High, Galic High and the Bohemian-Vindilician Range, the basin was almost completely locked except short-term existing narrow straits to the Neo-Tethys (NT). Accordingly, most close to the sea level, cyclicity of the basin deposits developed by manifold scale and lithofacies, so that biostratigraphic correlation with standard sections has remained poor [37] [38].

The general topography provides a subdivision in basin (pelite-evaporate cycles), confined braid plains/alluvial fan of restricted extension (siliciclastics) and source areas (Paleozoic igneous, metamorphic and sedimentary rocks).

Figure 6 presents the lithostratigraphic column of the Upper Triassic (Keuper) based on the Stratigraphic Commission Chart of Germany (2017), [15] with special regard to the time-span from Carnian base (225 Ma) to the TJB (201 Ma); the siliciclastic formations (K2, K4, K5, K6.1, K6.2) are of high energy origin and cover the flat-dipping slopes of the basin.

Methodologically, we apply the procedure used in our last paper on the Permian Triassic boundary (PTB) where cyclic flash flooding during negative climate forcing was followed by semiarid/arid phases under positive climate forcing (SBs, hiatus, paleosol) relating to the Siberian LIP- and Neo-Tethys rifting/degassing [9] [11] [12].

Focusing on "indirect effects" caused by volcanism [7] [8] [9] [27] on the Carnian Stuttgart F. and on the Rhaetian Weser F. (K6.3) as well as by multiple impacting [10] [21] [22] [23] on the Norian Arnstadt F. (K5, K6.1) and the Rhaetian Exter F. (K6.2, K6.3), the siliciclastic deposits are shortly characterized with sedimentologic key patterns (nomenclature see appendix).

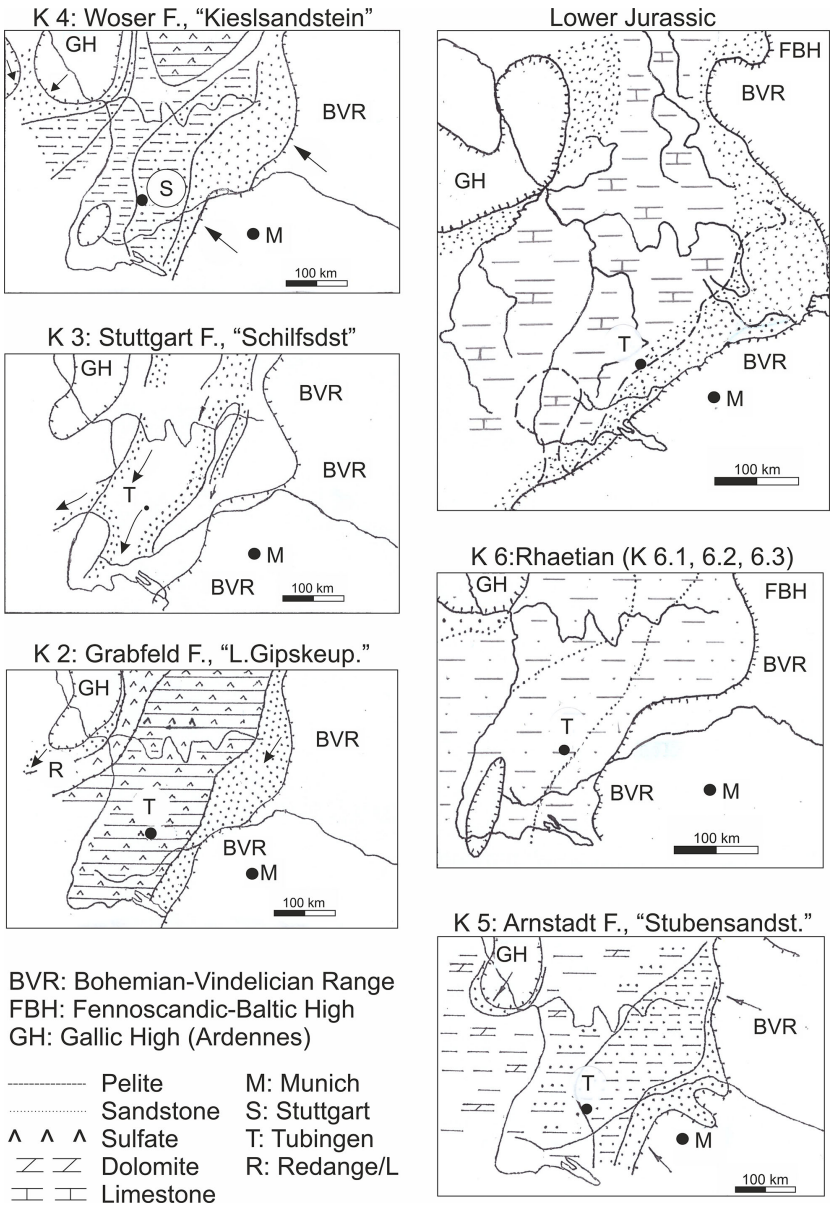

Figure 5. Paleogeographic sketches of the Upper Triassic F. (Keuper), Germanic Basin [37]: K2 Grabfeld F., K4 Exter F. (Rhaetian), Lower Jurassic. All formations are separated from each other by unconformities.

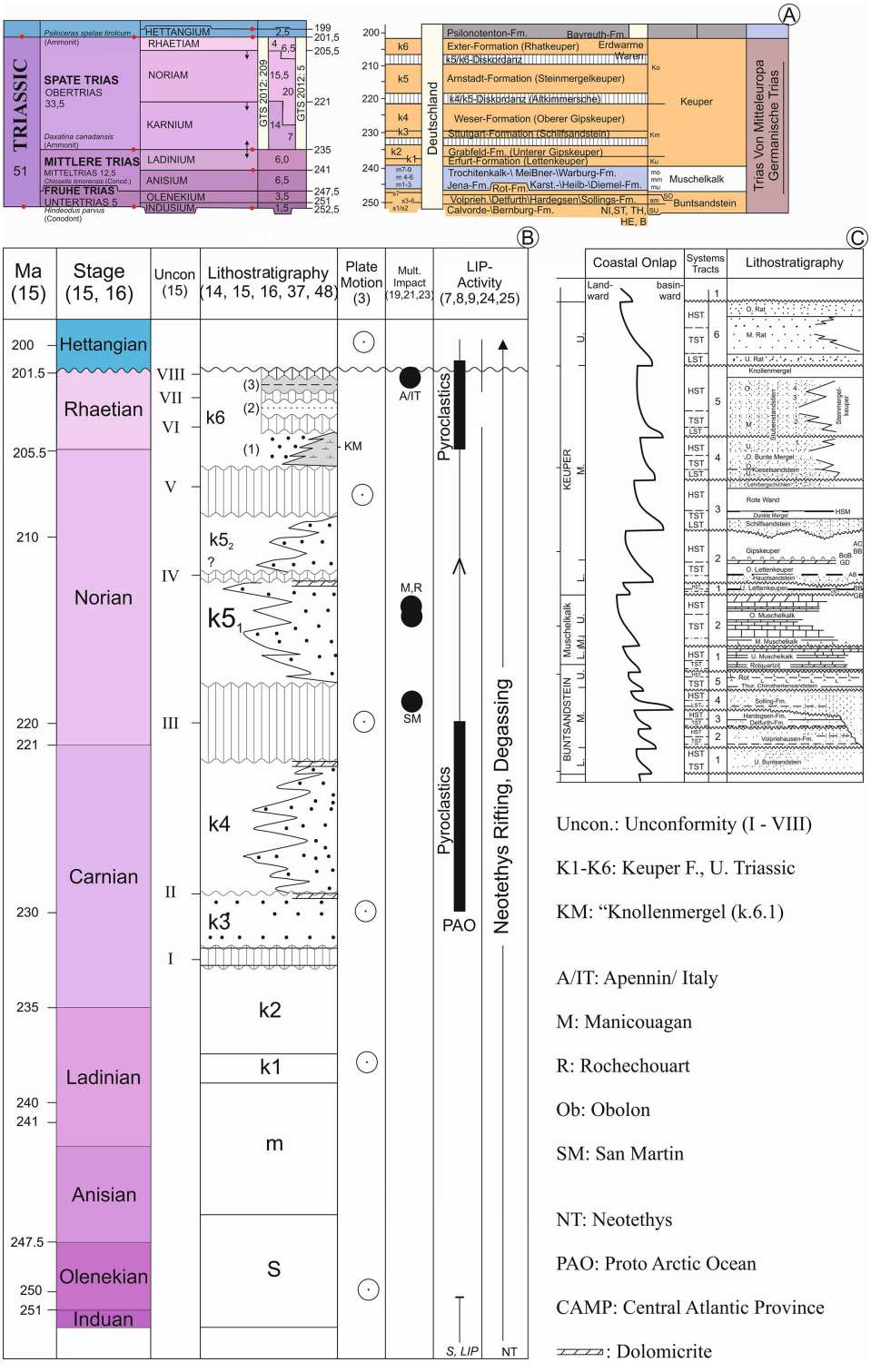

Uncon.: Unconformity (I - VIII)

K1-K6: Keuper F., U. Triassic

KM: "Knollenmergel (k.6.1)

A/IT: Apennin/ Italy

M: Manicouagan

R: Rochechouart

Ob: Obolon

SM: San Martin

NT: Neotethys

PAO: Proto Arctic Ocean

CAMP: Central Atlantic Province

: Dolomicrite

Figure 6. Strategraphy of the Germanic Basin (Germany 2017, Potsdam (GFZ)). A: Global Stratigraphy including GSSPs and Regional Stratigraphy [14] [15] [16] (Table). B: Lithostratigraphy of the Upper Triassic (Keuper) in the SE Germanic Basin; temporal relation to plate motion, multiple impacting and LIP-activity. C: Sequence analysis of the Triassic in the SW Germanic Basin (49). s: Lower Triassic, m: Middle Triassic, K1-6: Upper Triassic. LST: Low Stand System Tract, TSS: Transgressive System Tract, MFS: Maximum Flooding Surface, HST: High Stand System Tract.

Carnian: Stuttgart F. (K3) "SCHILFSANDSTEIN" (231.5 - 229.0 Ma) (Figure 7).

The 0 - 50 m thick sequence runs along a transform fault system from the Fennoscandic-Baltic High across the Germanic Basin NNE-SSW towards the Tethys. The braided river system, 5 - 15 km in width, exhibits major channels and paleo-valleys, 500 - 1000 m in width and up to 40 m deep, causing a paleorelief in the underlying Grabfeld F. (K2) and overbank fines with manifold pedogenic overprint [14] [37]. The fine- to coarse-grained siliciclastics are of greywacke/arkosic composition and expose all typical architectural elements and lithofacies types of fluvial environments based on [39]. They bear wood remnants (up to 12 m long silicified trunks), Equisetes sp., vertebrates (Phytosaurus, Therapods) and megaspores.

An intercalated, only regionally encountered sequence of multicolored pelite and dolomicrite (Gaildorf beds) indicates oxygen-deficient conditions in a brackish environment (pH > 7) owing poor fossil content (ostracods, bivalves, gastropods). Obviously, an abrupt intraformational climate change from humid/warm to arid/warm occurred.

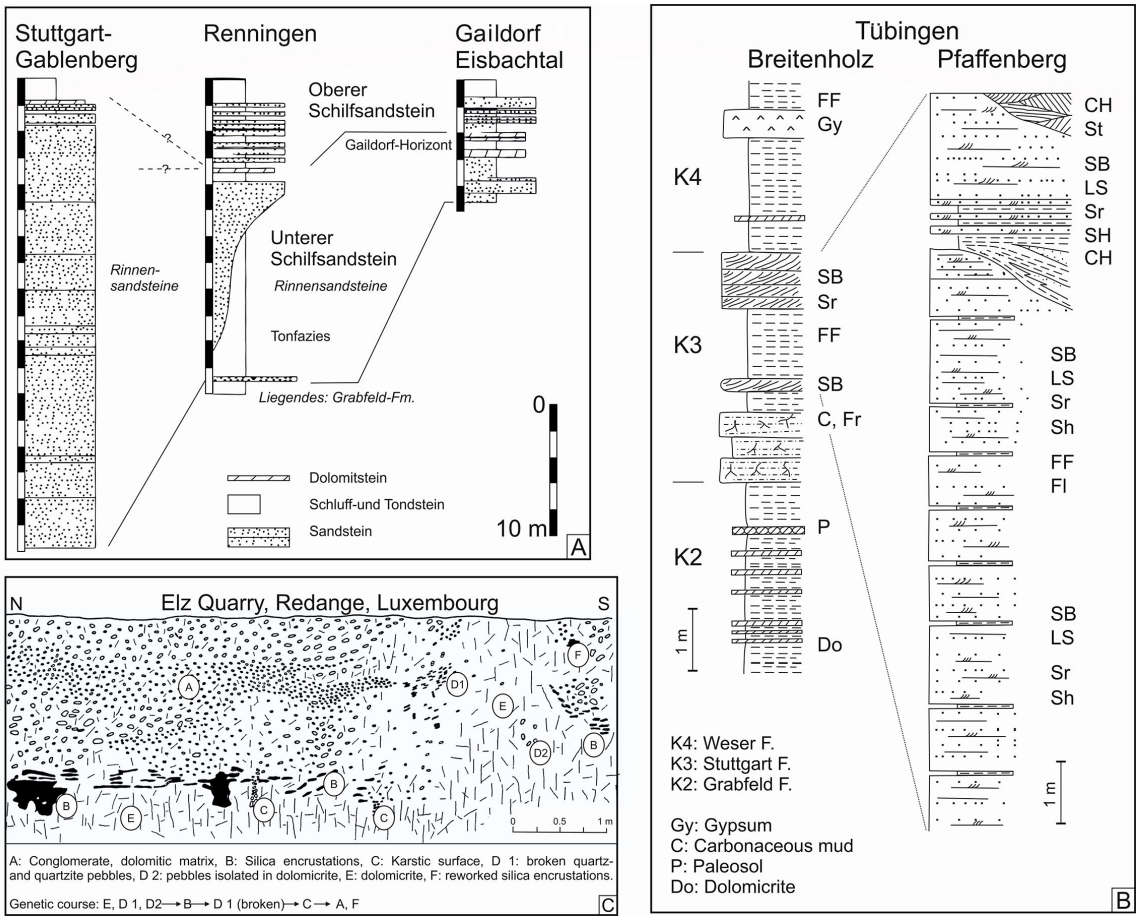

Figure 7. Architectural elements and lithofacies types [39] of the Stuttgart F., K3, "Schilfsandstein" [14] [15] [16]. A: Stuttgart area, B: Tübingen area [18], C: Southern margin of the Gallic High, Luxemburg, siliciclastic/dolomite cycles [40] probably part of the Grabfeld F. K2 below the unconformity to K3.

Accordingly, the foreland of the Gallic High/Ardennes Mts. (Luxembourg) represents during the same time-span (Grabfeld/Stuttgart/Weeser F.) a cyclic sedimentation of high-energy fluvial gravel deposits (Gm!) and early diagenetic playa dolomicrite [40], (**Figure 7C**).

Upper Carnian: Weser F./Hassberg F. (K4) "Kieselsandstein" (229.0 - 221.50 Ma)

This formation exposes basin deposits (pelite, dolomite, sulfate): (**Figure 8C**) and siliciclastics (Hassberg F.). The latter dominate marginal braid plains fed by the Vindelician-Bohemian source areas, thinning out towards the basin center. The coarse-grained, poorly sorted arkosic sandstone owns low maturity and builds up confined braid plains and alluvial fans exhibiting proximal amalgamated channel fills, sheet flood deposits and overbank fines [37] [41], (**Figure 8A**, **Figure 8B**).

The Hassberg F. is intercalated with a ~10 m thick pelite of restricted occurrences (eroded?) exposing on top pedogenic carbonate/sulfate encrustations and concretions indicating a hiatus and climate change comparable with the K3 F.

In case of high thickness, the amalgamated sequence yields at least four cycles without fining upward features because of the short and fast chaotic mass flow transport.

Paleontological finds are presented by plant remnants, silicified wood, sauria and invertebrate trace fossils and the fresh water crab Triops concriformis [37].

Norian: Arnstadt F. (K5), "Stubensandstein, Steinmergellkeuper" (218 - 209 Ma), (Figure 9, Figure 10)

This formation also reveals a broad variation of thickness (10 - 80 m) following on the hiatus K4/K5 (221.5 - 218 Ma), and exhibits four main siliciclastics cycles [14] [16] [37] [42].

The fine- to coarse-grained siliciclastics (arkosic sandstone, pelite) of low maturity, were deposited via fluvial/mass flow transport on alluvial and confined braid plains, where sheet floods, major channels (partly amalgamated fills) interfinger with overbank fines and playa deposits (pelite, carbonate rocks). Architectural elements and lithofacies types comprise the complete fluvial spectrum [37] [39] [42]. However, all top portions of the four main cycles developed paleosols/pedogenetic overprint in form of encrustations (calcite, dolomite) and concretions as well as dolomite beds up to 3 m in total thickness [14], more or less eroded by the next siliciclastic cycle.

That tells: Each cycle comprises a fast change from humid/warm to arid/warm climate conditions. So some 20 minor flash flood cycles maybe counted in one of the four upper cycles; compare similar processing in the Upper Permian Um Irna F., Jordanian Platform [29] [30] [31] [32] [33].

Kaolinite, sudoite (=dioctaedric chlorite), and diverse mixed layer minerals characterize the clay mineral assemblage [42] [43], whereby sudoite remains stable under increased temperature and pH > 7 versus kaolinite.

Fossils in the ciliciclastics: Sauria, turtles, batrachians, fishes, conchostraca, ostracoda, trace fossils, plant fragments [14].

Fossils in carbonate rocks: Molluscs (Unio sp.), gastropods?

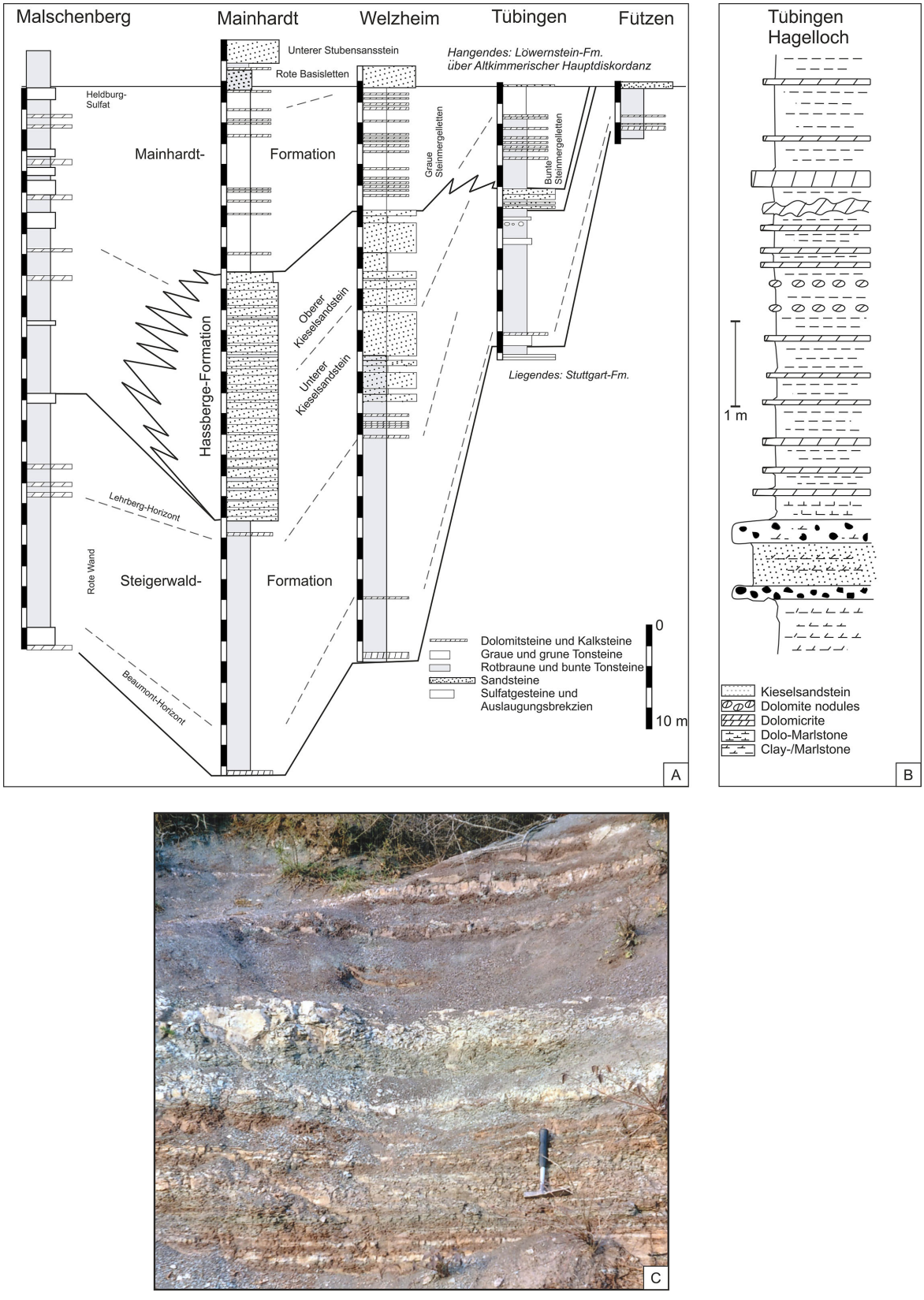

Figure 8. Lithofacies section of the Weser F., K4, "Kieselsandstein", A: Stuttgart area [14] [15] [16], B: Tübingen area [14] [18], C: Section Breitenholz, Tübingen area showing multicolored pelite and intercalated dolomicrite beds thereby missing the "Kieselsandstein", see arrow! [18].

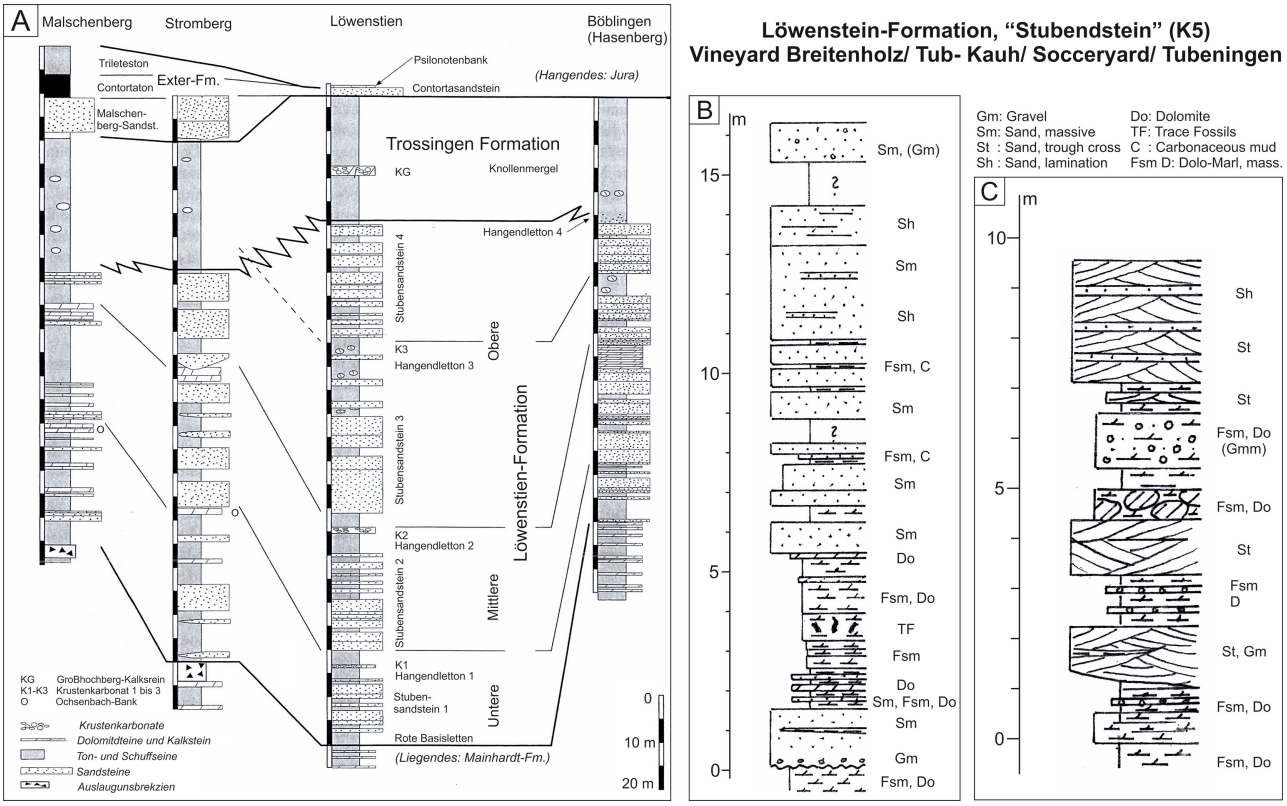

Figure 9. Lithofacies cycles of the Arnstadt/ Löwenstein F., K5 "Stubensandstein". A: Stuttgart area [14] [15] [16]; the overlying Trossingen F., K6.1 massive "Knollenmergel" represents the Norian/Rhaetian transition. B: Tübingen area [18].

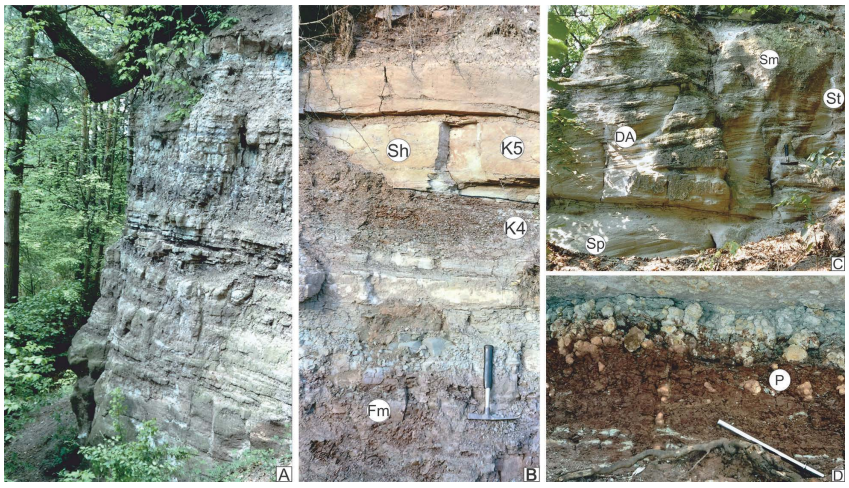

Figure 10. Outcrop of the Löwenstein F., K5, "Stubensandstein", Ammerbuch/Tübingen area (A-D). A: Alternating sandstein-pelite-dolomite cycles overlying a basinal high energy sandstone (Sm, Sh), Schönbuchspitz (W. Kost), Entringen, B: Main unconformity separating pelite and marly dolomite (K4) from the overlying flash flood deposits (K5), Weinsteige Breitenholz. C: Basinal high energy siliciclastics (Sm, Sb) as initial event of the K5 F., Schönbuchspitz, Entringen. D: Paleosol (dolomite nodules) atop of the K4 F., directly below K4/Ks unconformity, Vineyard Unterjesingen, Tübingen area.

The lower Norian matches the time-span of multiple impacting (220 - 214 Ma) [19] [21] [22].

Rhaetian: Exter F. (K6), Postera = Contorta-Triletes Beds, (205.5 - 201.5 Ma)

Across Germany, the Rhaetian developed above the K5/K6-unconformity (Figure 6).

Lower Rhaetian (K6,1) Postera, "Knollenmergel" (=Nodular Marlstone) (Figure 11)

In S Germany, the "Malschenberg-facies" is built up with interbedded sandstone, multicolored pelite and fossil-poor dolomicrite, locally pedogenic overprint [12] [13] [14]. Bivalve (Unio sp.) and fish remnants indicate a brackish environment. Because of the fast facies change, erratic origin and discordance, the stratigraphic relation to the so-called "Knollenmergel"-facies remains uncertain. This unusual clayey formation interfingers the top-portion of the third main Norian siliciclastics cycle with a thickness of 0 to 70 m!, also called "Trossingen F.", famous by finds of land-derived fossils including dinosaurians [14].

The red-brown silty structure-less clay stone contains irregularly scattered carbonate nodules/encrustation fragments of early diagenetic or reworked origin and single quartz grains [14] [44]. Clay minerals as dioctaedric regular mixed layer (sudoite-vermiculite-montmorillonite 001 = 31 Å) and sudoite (=dioctaedric chlorite) contribute ~30% montmorillonite (A4), a reason for landslides and bad construction ground.

Because of missing sedimentary structures, the genesis of this facies has been commonly interpreted as of "eolian provenance" during hazardous storms that eroded parts of the underlying sequence [14] or as a kind of mudflow to be derived from a Paleozoic volcanic formation cropping out in the Vindelician-Bohemian source area [44]. But its age corresponds with the NT- and PAO-rifting, especially with a kimberlitic pyroclastic eruption in the latter rift-zone [7].

In a restricted area of SW Germany, ("Mittelbronn beds") at Schwäb Hall, this massive clay stone is overlain with fossiliferous dolomicrite beds and grey-violet pelite bearing pyrite concretions: pH < 7 and coal seams deposited in isolated playas [14].

In the eastern Subhercynian Basin/ N Germany, the Postera beds expose fluvial/deltaic siliciclastics mainly derived from the Fennoscandic High. A main channel system at loc. Hedeper [45] [46] interfingers westward with grey-green pelite of the basin; of special interest is a 1 m thick tuff-suspicious "green boundary clay".

Ostracods for biostratigraphic subdivision [48] and bivalves (Unionites posterus) underline a brackish environment.

Middle Rhaetian (K6.2) Contorta Beds (Figure 12)

In SW Germany, the Contorta beds overlie the "Knollenmergel" (K6.1) or the Arnstadt F. with a sharp unconformity. In total ~8 m black shale and ~12 m quartz arenite without any carbonate content interrelate with each other. A rich mollusc fauna (e.g. Rhaetavicula contorta) predominates, accompanied by trace fossils and cyclic bioturbation in an intertidal environment [18] [45] [46] [47] [48].

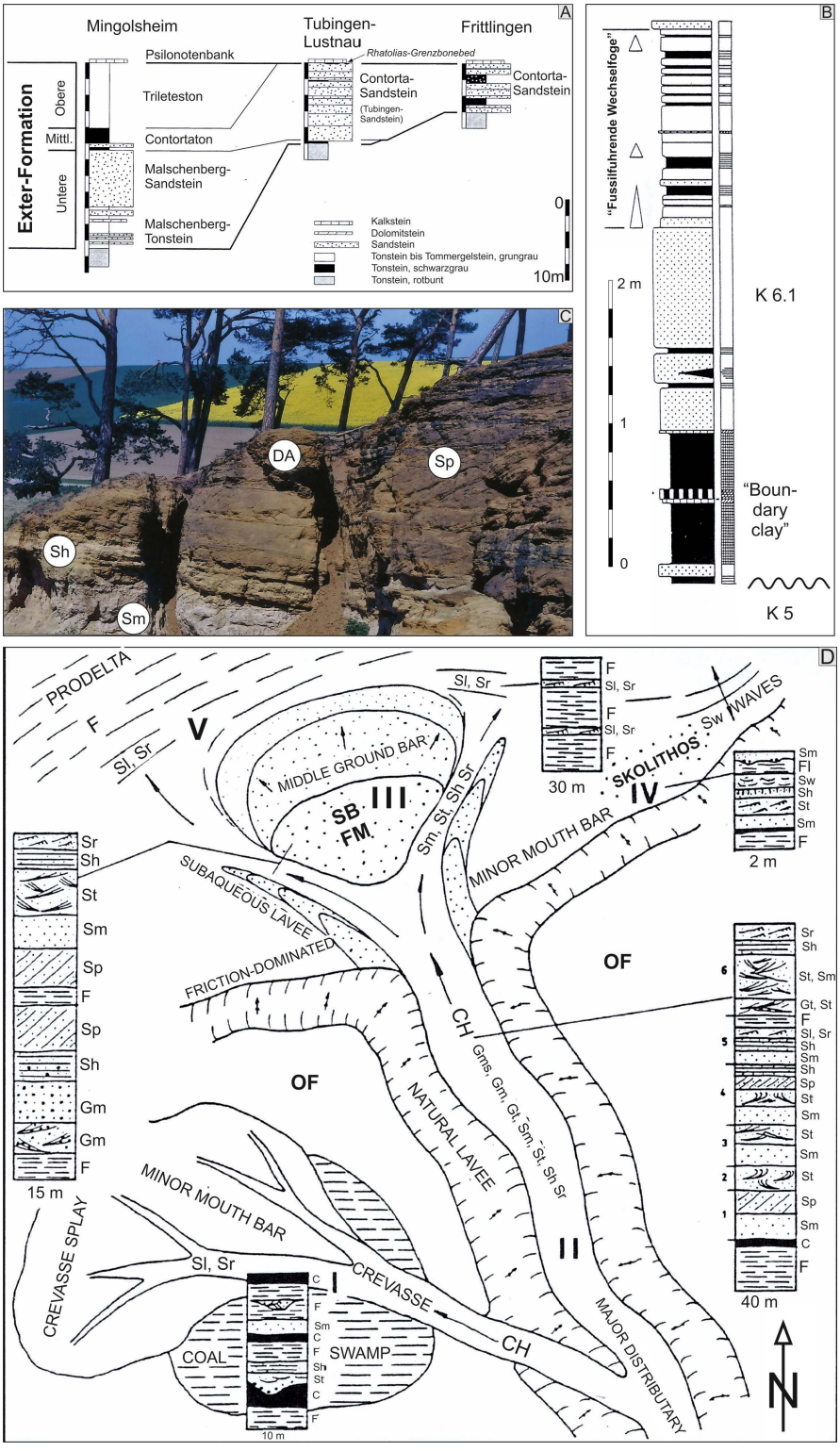

Figure 11. Lower Rhaetian, K6.1, Exter F. A: Lithostratigraphy of the Exter F. in the SW Germanic Basin [14]. B: Transitional lithofacies of the Lower Rhaetian, K6.1, Seinstedt Section, Subhercynian, N Germany [47]. Note the boundary claystone at the base! C: Deltaic channel fill course-grained siliciclastics (DA: Sp, SH) of the K6.1 F., Hedeper Section, Subhercynian, N Germany [45] [46] [47]. D: Model of the deltaic transitional zone of the K6.1 F. for the Hedeper/Seinstadt area, Subhercynian nomenclature [39].

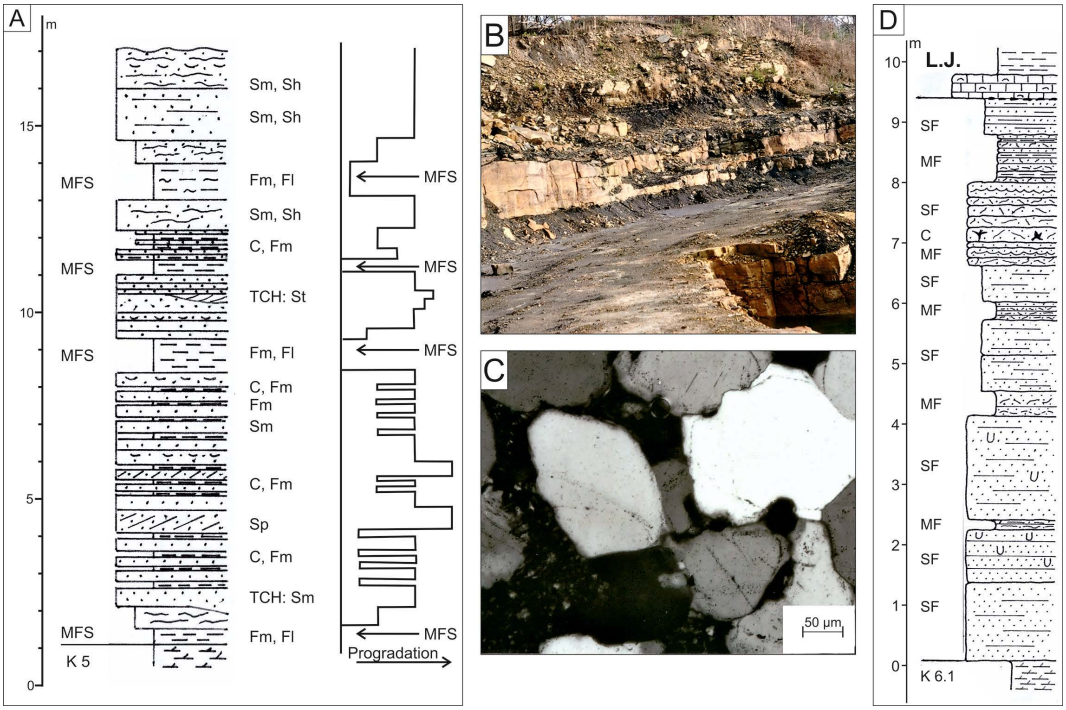

Figure 12. Middle Rhaetian Contorta Beds, K6.2, Exter F. A: Lithofacies of intertidal/subtidal siliciclastics bearing trace fossils; the prograding quartz arenite is interbedded with black shale facies interpreted as MFS, shrinkage cracks by synaeresis caused by salinity change, Quarry Körner,Velpke, Subhercynian. B: Quarry in the Contorta Beds, Velpke, Subhercynian, N Germany: Alternating prograding quartz arenite of high maturity with transgressive oxygen-deficient black pelite. C: Quartz arenite, kaolinite/illite matrix, partial syntaxial overgrowth followed by pressure solution, resediment: thin section, crossed-nicols. D: Comparable section in the Contorta Beds at Bebenhausen/Tübingen, SW Germanic Basin. Dominance of quartz arenite without interbedded pelite, intertidal/subtidal environment, endobenthos: Diplocraterion sp.

In the Subhercynian Basin, N Germany a similar lithofacies bearing forams and bivalves covers deltaic/ intertidal plains built up with quartz arenite of high maturity that interfingers with black shale [18] [45] [46] [48].

Of specific interest appears the siliciclastic mineral assemblage' reduction through the Lower to Middle Rhaetian changing from arkosic/subarkosic composition—by the loss of feldspar and unstable heavy minerals (garnet, hornblende epidote) [45] [46]—to quartz arenite under the same source area. Eh and pH underlie significant variations during this time-span.

Upper Rhaetian (H6.3), Triletes Beds

Through N and SW Germany the 0 - 12 m thick carbonate- and almost fossil-free, grey-green pelite sequence was deposited in a brackish environment according to ostracods [48], plant remnants and megaspores of Triletes sp. [47] [48]. However, missing carbonates and faunal scarcity indicate acidification.

This formation was regionally eroded (K6.3) (J-unconformity) and finally covered by the first ammonite-bearing Hettangian carbonate rocks (Psiloceras psilonotum) [14].

The time-span from Carnian to TJB is characterized by continuous NT-, PAO- and CAMP-rifting degassing with special focus on kimberlitic pyroclastic erup-

tions (PAO) through the Carnian (K3, K4) and Rhaetian (K6) [7] [25] [27].

Common/uncommon sedimentological key patterns of the Upper Triassic F. in the Germanic Basin

- The Formations (K3, K4, K5, K6.1) are separated by 6 unconformities covering ~ 30 Ma (231.5 - 201.5), (**Figure 6** [49] [50], **Table 3**).

- Above each unconformity abruptly follows high energy siliciclastic deposition possibly matching plate motion [3].

- The subarkosic/arkosic clastics are of fluvial, mass flow and flash flood origin deposited on alluvial fans and confined braid plains; they represent a marginal facies caused by hazardous atmospheric events and interfinger with basin deposits (pelite, dolomite, evaporates).

-The mass flows relate to liquefied/fluidized transport processing, hitherto applied to subaquatic clastics [51] (**Figure 13**): thereby, re-sedimentary processes develop from elastic—via plastic to viscose—fluidal flowing state between proximal to distal destinations.

- The siliciclastic sequences built up with several minor cycles are finally topped with pedogenic carbonate encrustations and/or playa pelite/dolomicrite deposits, however, often eroded. Such cycles indicate change from humid/warm (pH < 7) to semiarid/arid conditions (pH > 7).

- Oxygen-deficient pelite and interbedded coalified wood remnants evidence a fast change of pH, Eh and T comprising wildfires? Compare [52].

The clay mineral assemblages are commonly characterized by kaolinite, illite and irregular illite/montmorillonite mixed layers. However, the Norian (K5: "Stubensandstein", "Knollenmergel") and the Rhaetian (K6: Exter F.) contain striking amounts of sudoite and sudoite/montmorillonite mixed layers [42] [43] [44]. This time-span comprises multiple impacting [18] [20] [21] [22] and rift-magmatism/degassing [7] [8] [9] [11] [12] [25] [26].

- Furthermore, other evaporate-bearing pelites expose regular chlorite-smectite mixed layer minerals [53] [54]. **Figure 14** [55], compiles the clay mineral assemblage of Upper Triassic/Jurassic pelites in N Germany.

The maturity-change of subarkosic clastics deposited from the K6.1-Postera Beds to the K6.2 Contorta Beds (loss of feldspar and unstable heavy minerals) under the same source area and the resulting formation of interbedded quartz arenite/anoxic pelite differs from all other Upper Triassic Formations.

Table 3. Change of Earth-Moon Data [57] [59] [60] [61].

Age (Ma)	Earth-Moon distance (km)	Moon's Recession Rate (km/Ma)	Earth's Rotational History Days/Month	Days/year
153	381,907	18.66	30.15	376
220[a]	380,657	50.76	29.66	371.6
290	377,104	110.31	30.16	383

a MFS TR 70 a, plate motion, maximum opening of PAO, San Martin impact, base of "amalgamated paleosol", overregional unconformity in the Germanic Basin, mass extinction.

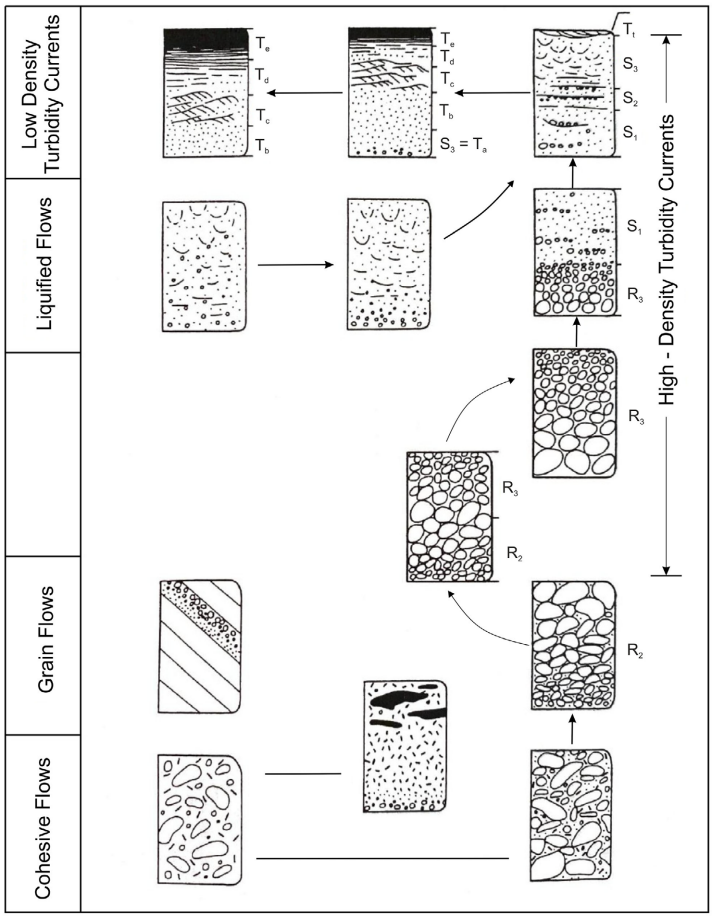

Figure 13. Stow's model for submarine flow [51] applied to the flash flood deposits of the Upper Triassic (Keuper) in the SW Germanic Basin.

- Based on the applied patterns, the Keuper sequence may be well understood by Event Stratigraphy [49] [50].

- $\partial^{13}C$- and $^{87}Sr/^{86}Sr$-Excursion through the Upper Triassic German Basin [56]

Along the isotope curves, the "data groups" reveal interruptions and dislocations through the complete Triassic sequence (**Figure 15A**, **Figure 15B**).

The analytical gaps meet the unconformities encountered in the German Basin [15] (**Figure 6**). Certainly, most of the top portions of the cycles were partially eroded, reworked, and shed by the next overlying mass flow into the basin center.

Using the $\partial^{13}C$-isotope data for correlation, the "data groups" also meet changes of sedimentary patterns and possible drivers (LIPs, impacts).

- Ladinian, Carnian, Grabfeld F. (K2):

Prior to the K2/K3-unconformity, the last "data group" meets after MFS Tr 50-ceasing during regression (RST) on the Arabian Shelf an evaporate phase (→SB).

- Carnian, Stuttgart F., "Schilfsandstein" (K3): The "data group" coincides with plate motion [3], NT- and PAO-rifting accompanied by kimberlite pyroclastic eruption [7].

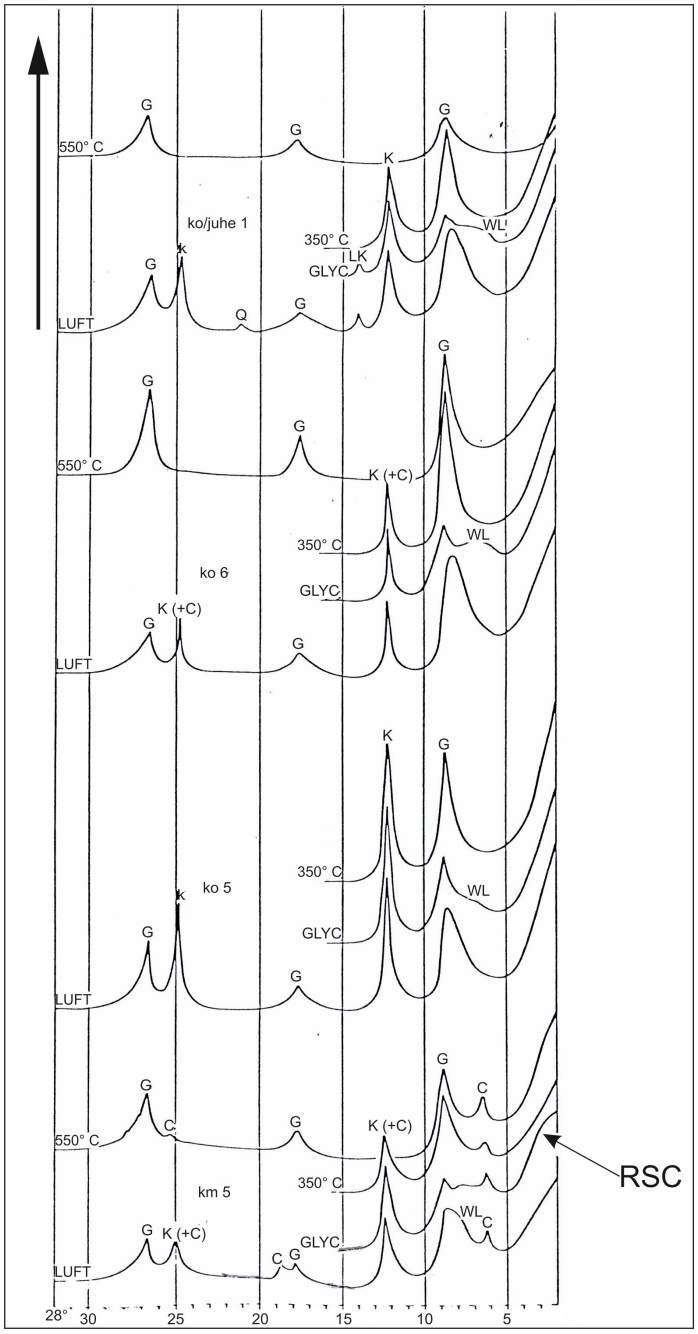

Figure 14. XRD-curves of clay mineral assemblages (<2 μm diameter) from the Norian, Rhaetian and Hettangian of the Subhercynian, N Germany [55]. C dioctaedric/triotraedric chlorite, G. illite, WI irregular illite/smectite mixer layer, K kaolinite, BSC regular smectite/chlorite mixed layer (001 ~ 31 Å).

- Carnian, Weser F., "Kieselsandstein" (K4):

Two separated "data groups" match plate motion [3], both MFS Tr 60 and Tr 70a, PAO-rifting and its continued pyroclastic eruption [7].

- Lower Norian, Arnstadt F., "Stubensandstein" (K5.1):

A uniform "data group" meets the amalgamated MFSs Tr 70a,b,c, PAO-rifting and the San Martin impact [19] [21] up to unconformity K4/K5.1.

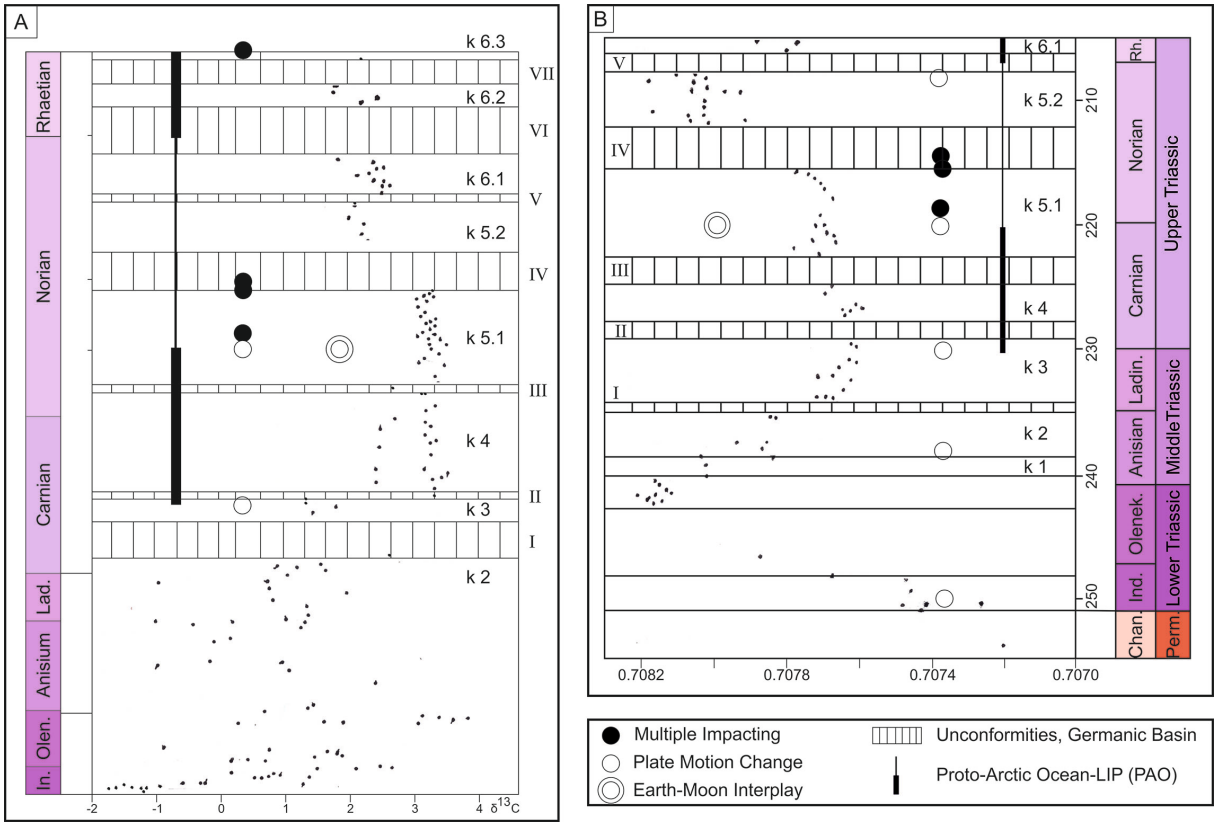

Figure 15. Isotope data of the Triassic [56] relating to the Event-Stratigraphy in the SW Germanic Basin [15] [16], plate motion [3], multiple impacting [19] [21] [23] and LIP activity [7] [8] [9]: A: $\partial^{13}C$, B: $^{87}Sr/^{86}Sr$. Note the gaps and "dislocation" of data group along the time line. ∂13C: whole rock, $^{87}Sr/^{86}Sr$: conodonts.

- Upper Norian, Arnstadt F., "Stubensandstein" (K5.2):

Significant dislocation of "data group" towards lower values ($\partial^{13}C$: (3.5 → 2) after multiple impacting (Manicouagan, Rochechouart, Obolon) during the K5.1/K5.2-unconformity, amalgamated MFSs Tr 80a,b, NT-/PAO-rifting and clay mineral change (sudoite, mixed layer) [42] [43] [44].

- Lower Rhaetian, Exter F., Postera beds, "Knollenmergel", K6.1:

Dislocated uniform "data group" after the K5.2/K6.1-unconformity: Plate motion, continued rifting (NT < PAO), kimberlite pyroclastic eruption, striking clay mineral change (sudoite, smectite-bearing mixed layer) [44].

- Middle Rhaetian, Exter F., Contorta beds (K6.2):

Less isotope data after the K6.1/K6.2 unconformity, continuation of NT- and PAO-rifting/degassing, increase of acidification [14] [48].

- Upper Rhaetian, Exter F., Triletes beds (K6.3):

High LIP-activity (PAO, CAMP) and impacting [19] [23], lack of isotope data, acidification.

The "amalgamated paleosol" on the Jordanian Platform developed since the K4/K5-unconformity (San Martin impact: ~219 Ma) with a uniform $\partial^{13}C$-data group and the following excursions up to the TJB, comprising multiple impacting (K5.1/K5.2) unconformity (~211 Ma) and increasing aridity (evaporates of the Ruweis F. **Figure 3**) [15A].

The $^{87}Sr/^{86}Sr$ track exhibits two distinct minima: the Siberian LIP (0.7072) and the CAMP-LIP/TJB (7078). Maxima fall in the Upper Olenekium and into the Rhaetian (~0.7082). Between both maxima, the curve varies around a middle level (~0.7077).

5. Earth-Moon Meteorite Interplay: Consequences for Upper Triassic Sedimentary Processing (Figure 16)

Geodynamic aspects:

As generally accepted [57] [58] [59] [60] and applied in a feedback system [60], changes in Earth's mantle rotational energy have potential influence on triggering activity at the core/mantle boundary and on other material transport in convection cells of the deeper mantle [59] [60] [61], (**Table 3**) as being an essential source for LIPs and MOBs. During magmatic activity Earth's rotation slows down causing a normally polarized magnetic field and vice versa. That is combined with sea level rise (tidal dissiptation [61]) and with negative climate forcing realized by atmospheric hazard on land (flash flooding) [29] and MFSs in sea (oxygen-deficient shale) [25].

A significant change of both Moon's recession rate (50.76 → 18.66 km/Ma) and Earth's rotation velocity (29.66 → 30.15 days/month) took place ~220 Ma [57] [60]. This was the time when multiple impacting aroused [19] [20] and NT-[25]/PAO-rifting [7], plate motion [3], "amalgamated" paleosol formation on the Jordanian Platform [34], and several unconformities in the Germanic Basin [15] (**Table 4**) took place.

Apart from the Carnian/Norian boundary mass extinction [62] [63], the "amalgamated" MFSs Tr 70a,b,c,-cycles [25] and the clay mineral assemblage in both study areas became obvious [34] [42] [43] [44] [53] [54].

Table 3 lists up the unconformities encountered through the Carnian to Norian time-span in the Germanic Basin in connection with the MFSs on the Arabian Shelf and magmatic drivers (NT, PAO).

Indicative for the LIP/MORB-frequency are the MFSs intervals (SBs): time-span between Tr 30 to Tr 60, which vary from 7 - 9 Ma while the interval Tr 60 to Tr 70 reveals ~5 Ma, probably affected by the ~220 Ma events. The lateral extension of the MFSs (tidal dissiptation) relates to the intensity of rifting (magmatic volume).

"Amalgamated" MFSs expose different intervals (**Figure 4A**):

- Tr 10 to Tr 30 (Induan): ~2.0 - 1.0 Ma directed by tailings of the Siberian LIP [29].

- Tr 70a,b,c (Norian): 3 - 3.5 Ma coinciding within the ~220 Ma event [19] [21].

- Tr 80a,b (Upper Norian): ~4 - 5 Ma, NT-PAO-rifting, multiple impacting.

- The Arnstadt F. (K5)/Germanic Basin (~218 - 209 Ma) exhibits four main cycles, each of them ~2.5 Ma subdivided in one to three minor cycles (~0.75 to 2.5 Ma/cycle) to be related to both PAO-rifting [7] and multiple impacting [19] [21].

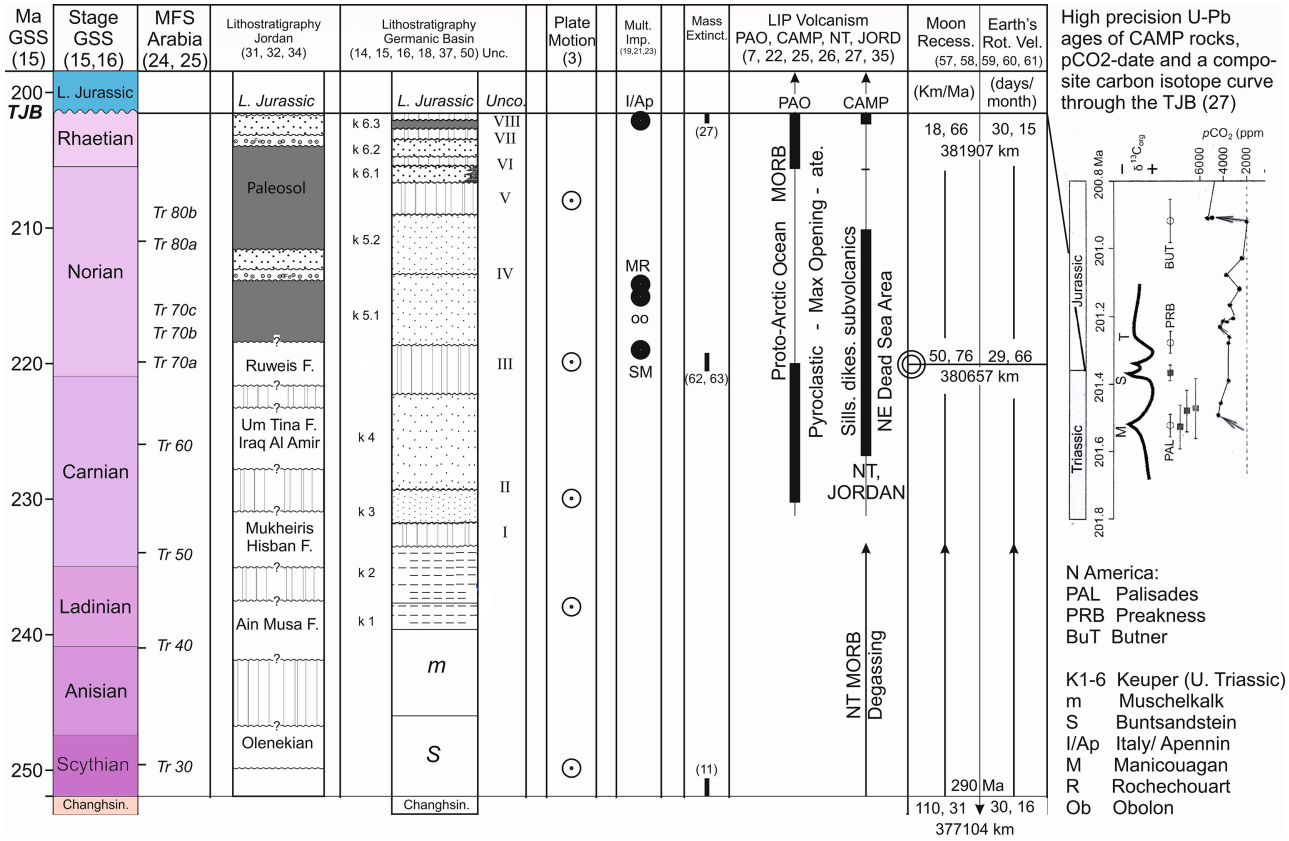

Figure 16. Compositional chart of the Triassic with regard to the Jordanian Platform, the Arabian Shelf, and the Germanic Basin. Drivers: LIP activity, multiple impacting, plate motion, and Moon-Earth relation. Effects: Climate forcing architectural sedimentary elements, lithofacies, Mg/Ca ratio, MFS/SB, event-stratigraphy, paleosols formation (clay mineralogy), mass extinction.

Table 4. Upper Triassic unconformities in Jordan/Germanic Basin and relating drivers/causes.

Boundaries/ Unconformities, Age (Ma) [15] [16]	Jordanian Platform [24] [25] [31] [32] [33] [34]	Drivers, events, causes [7] [19] [21] [22] [23] [27] [35] [60] [61] [77] [79] [80]
K6.3/Hettangian (TJB: 201.4 Ma)	Jurassic transgression above amalgamated paleosol	PAO-, NT-, CAMP-rifting/magmatism, mass extinction, Moon/Earth data ch.
K6.2/K6.3	Amalgamated paleosol	PAO-pyroclastic eruption, acidification, CAMP-activity, PDS in quartz
K6.1/K6.2	Amalgamated paleosol	NT-magmatism, PAO-pyroclastics
K5.2/K6.1 (209 - 206.5)	Amalgamated paleosol, Dead Sea subvolcanics, Tr 80a,b	Upwelling asthenosphere (Ivrea), NT-, PAO-magmatism, plate motion
K5.1/K5.2	Amalgamated paleosol, continuation of Tr 70b,c, Dead Sea subvolcanic suite	Multiple impacting (Manicouagan, Rochechouart, Obolon), plate motion
K4/K5.1 (219.5 - 211.5)	Tr 70a, base of amalgamated paleosol	San Martin impact, NT-rifting, mass extinction, change of Earth-Moon data
K3/K4	NT-rifting, increase of Mg/Ca ratio (dolomite)	First PAO pyroclastic eruptions, plate motion
K2/K3 (233 - 231.5)	TR 50	End of Siberian LIP, plate motion

Revisiting the Triassic Chart [25] (**Figure 4A**), all MFSs show a kind of asymmetry with regard to the TST/RST: a fast growth of the MFS (pelite, black shale):

(0.1 - 1.0 Ma) and a retardation during the regressive phase (dolomite, evaporate → clastics) back to the following SB; all in all representing the duration of LIP-activity and climate change from humid/warm (negative climate impacting) to arid/warm (positive climate forcing).

Regarding the Moon's influence on the LIP activity, astronomical tuning should be a subject in this geodynamic scenery as already applied through the Lower Triassic in connection with the Siberian LIP [64].

Mineralogical implications

- Siliciclastics: in the Germanic Basin, the primary arkosic/subarkosic clastics of the source areas underwent a short transport without having been reworked, so keeping their primary mineral content and their low maturity (K3-K5).

However, the conditions changed at the Lower/Middle Rhaetian boundary (K6.1-K6.2) when hazardous acidic flash floods, increasing transport length and reworking on braid plains during a TST grew on to strongly reduce the unstable conditions of the primary mineral assemblage (feldspar, garnet, amphibole, epidote, biotite). The change to quartz arenite was sourced in the NT-, PAO- and CAMP-rifting/degassing.

- Siliciclastic-Pelite-Carbonate Cycles: Early diagenetic concretions/encrustations (calcite, dolomite) in paragenesis with red pelite (mostly in K5), indicate an arid/semiarid climate (pH > 7) after clastic tailings of flash flood events caused by major volcanic and impact events.

Interbedded dolomicrite (rarely fossiliferous) in oxygen-deficient grey, black or violet pelite overlying flash flood deposits (K3, K4, K5), were deposited in playa environments (pH > 7).

Despite of permanent arguments for early diagenetic origin [46] [65], a primary dolomite precipitation cannot be excluded [66] [67] [68]. Grey, black, violet, bituminous, even coal-bearing pelite, carbonate and fossil-free, has to be derived from acid/toxic rain during magmatic degassing (NT, PAO, CAMP) and tephra-bearing suspicious tuffite like the Upper Rhaetian pelite in Italy [23] bearing PDS in embedded quartz grains, overlying the Middle Rhaetian Rhaetavicula contorta beds.

- Clay minerals as event-indicators: Paleosol, "boundary clay": Across the Germanic Basin the clay mineral assemblage of the Upper Triassic sediments is commonly represented by kaolinite, illite and irregular illite/montmorillonite mixed layer minerals. While kaolinite originates as a weathering product of feldspar (kaolinized rims) under pH 4 - 6, illite generates by degradation (K^+) of both micas (muscovite, biotite) from the Paleozoic source areas [42] [43] [69].

However, some clay minerals' paragenesis significantly differ: The formations K1-K4 contain the regular chlorite-montmorillonite mixed layer mineral corrensite [42] [43] [53] [54] [69] in paragenesis with Mg-bearing evaporates (dolomite, sulfate). But smectite bearing pelite may contain tephra-portions of pyroclastic origin (volcanism, impacting) transformed into montmorillonite by pH > 7 [43] [69], see *i.e.* NT-, PAO-rifting.

The Norian Arnstadt F. (K5) contains sudoite (=dioctaedric chlorite), irregular kaolinite/sudoite mixed layer and tosudite (irregular/regular) mixed layers with montmorillonite portions [42] [43]; thereby sudoite remains stable under increased temperature (>350˚C) and under pH > 7 in contrast to kaolinite [43]; this may explain hot fallout of volcanic/impact origin.

The massive, structure-less Lower Rhaetian "Knollenmergel" (K5/K6-unconformity, K6.1) that interfingers with the siliciclastics of the Arnstadt F. (K5) is mainly composed of sudoite and a regular dioctaedric sudoite montmorillonite mixed layer mineral (001: 31 Å, 30% montmorillonite) [44]. As predominantly interpreted, pyroclastic tephra and other mineral/rock-glass transform under alkaline conditions to primary/secondary bentonite in combination with magmatic liquids and vapor [69].

In fact the "Knollenmergel" (Nodular marlstone) coincides with the kimberlite PAO-rifting [7] and may present a mixture of volcanic glass-bearing tephra and whirlstorm-reworked fine-grained regional red beds (K5). Because of the different age of multiple impacting (~219 - 214 Ma), a participation of impact-fallout appears rather less probable.

On the Jordanian Platform the Norian-Rhaetian "amalgamated paleosol" complex (**Figure 4B**) covers a time-span of 15 - 20 Ma and compromises at least three Fe-encrustation-bearing paleosols. The clay mineral assemblage of the structureless Units 1 and 3 reveals, apart from kaolinite and illite, irregular montmorillonite, illite and sudoite-montmorillonite mixed layer minerals (reinterpreted after: [32] [34]) and natroalunite. Thus, similarities do exist with relevant deposits in the Germanic Basin, however missing corrensite. Both sudoite and natroalunite (feldspar derived?) are stable > 350˚C and pH > 7 [69]. Are there portions of "boundary clay" hidden in this amalgamated sequence?

For comparison with the KPgB, in continental series, like the Raton Basin, New Mexico, Colorado, a white kaolinite layer (or dickite?) altered by hot impact fallout, is overlain with a coal bed composed of fusinite and macerated plants [70] [71]. The following clay stone contains iridium and other siderophile elements in a 10 cm thick interval [72], and PDS in quartz grain [73] [74] [75]. The interrelation between the maximum of siderophile elements and palynologic data gives hints on initial recolonization after devastation across the KPgB [71].

Thus, to meet all requirements for the proof of boundary clay (*i.e.* [70]), in both study areas we unfortunately miss all high resolution mineralogic/geochemical data concerning PDS in silicates (quartz, feldspar), impact/volcanic glass, microtectite, $\partial^{13}C$ and $^{87}Sr/^{86}Sr$ data, siderophile elements and palynologic data. However, the conditions to succeed in the future are promising.

Positive/negative climate forcing: Relevance to target areas

Oceanic LIPs and marine impacting cause tremendous volumes of replaced/vaporized sea water providing negative climate forcing accompanied by MFSs and flash flooding via atmospheric hazards (**Figure 16**). Simulation of the Chicxulub impact/KPgB boundary [76] [77] gives insight into a mixed process of

positive/negative climate forcing as encountered by ~100 m deep sea water, ~2900 m interbedded limestone, dolomite and sulfate rocks overlying ~T30 km granitic basement. So, we are faced with greenhouse gasses (CO_2, CH_4, CH_3Cl, CH_3Br, FCKW, NO_X: $+Wm^2$) resp., sulfate, aerosol, ozone depletion, smoke, clouding ($-Wm^2$), and a broad spectrum of shocked fallout [76] [77].

In case of the Upper Triassic continental impacting, the target areas comprise granitoids, anorthosite, and a broad variation of metamorphic rocks (**Table 2**); because of the prevailing silicate rocks one may expect a dominance of positive climate forcing ($+Wm^2$).

The prominent examples for continental KPgB impact was encountered in Raton Basin, New Mexico, Colorado and other areas in the N America [72] [73] [74] [75] offer an occasion how to approach the "boundary clay-suspicious" Upper Triassic structure-less clay formations in our both study areas.

$\partial^{13}C$ and $^{87}Sr/^{86}Sr$ isotope data relating to the driving forces

As already experienced across the PTB [29], in general, decreasing $\partial^{13}C$ values indicate negative climate forcing (MFSs) and vice versa initiate positive climate forcing (SBs):

From Induan to Lower Carnite a broad dissipitation of data-groups gives hint on several magmatic drivers of varying petrochemistry (Mantle/ Crust) [56].

From Middle Carnian to the TJB slight variations develop during NT-, PAO-, and CAMP-rifting/degassing contemporaneously with plate motion (**Table 1**, **Figure 16**); the latter increased since major PAO-opening.

Rise and fall of data-groups and their "dislocation" (data gaps) coincide with the unconformities in the Germanic Basin (**Figure 15**) and probably with the tephra degassing-ratio (negative/positive climate forcing).

As generally accepted *i.e.* [78], the $^{87}Sr/^{86}Sr$ ratio develops from deeper mantle rocks to crustal rocks and its sedimentary derivate from lower to higher values [9] [11] [56]: So the Siberian LIP association averages around 0.7074, followed by increasing crustal incorporation during the Olenekian to Anisian (0.7082) and to the Norian/Rhaetian boundary (0.7081); in between a long term middle level (0.7077) remains during varying intensity of NT-, PAO- and beginning CAMP-rifting [65].

Thus, the main driver directed the isotope data by the interplay of LIP activities, crustal assimilation, and contact metamorphism with meta-sedimentary rocks (oxygen-deficient pelite, black shale, evaporates, and hydrocarbon) [9] [11] [12].

6. Conclusions: Drivers and Triggered Sedimentologic Patterns

Despite the broad age error bars (**Table 2**), the interaction of endogenic drivers (LIP-, MORB-degassing: NT, PAO, CAMP) and Multiple Impacting with exogenic effects on sedimentary processing during the Upper Triassic, provides the following geodynamic/sedimentologic scenery (Comp. **Figure 16**):

The Upper Triassic subvolcanic suite located in the NE Dead Sea area exposing strongly alkaline character and enrichment of incompatible element patters (continental rift zone magmatism), has got a prominent analogy by the alkaline dike system in the northern Ivrea Zone, (Italy, Southern Alps).

The latter provinces' derivatives of a convecting asthenosphere whose upwelling started during the Anisian were followed by high volcanic tuff production/magmatism since the Ladinian/Carnian boundary. It was sourced in the Lower Crust/Upper Mantle transition zone in connection with metasomatic enrichment. That resulted in a long-term conductive heat transfer (~20 - 30 Ma) within the Crust [80] during the initial development of the Neo-Tethys.

LIP-/MORB activity directs climate forcing, plate motion, MFS/SB cycles, and $\partial^{13}C$, $^{87}Sr/^{86}Sr$ excursions.

Positive climate forcing causes increasing temperature and SBs, evaporation (dolomite, sulfate), pH > 7, paleosol formation during unconformities, arid/warm conditions, and clay mineral assemblages' change.

Table 5. Model for the interrelationship of geoscientific driving forces via positive/negative climate forcing with effects on sedimentary processing.

Climate forcing Wm^2 [13]	Driving forces	Effects	
		Marine environment	Continental environment
Positive		Regressive System Track (RST)	Arkosic siliciclastics, eolianite
NO_x (0.2)		Sequence B. (SB)	Carbonates, evaporates in lakes, tuffite
FCHC (0.2)		Carbonates, evaporates on plate.	Smectite, pH > 7
CH_4 (0.3)		Unconformity, Hiatus	Calcimorphic soils
CO_2 (1.3)		Acidification	Ferrigenous soils
Solar radiation + 2.2	Magmatic degassing	Increasing $\partial^{13}C$	Fast facies change
	• Large Igneous Provinces LIP		Unconformity, Hiatus
	• Mid-Oceanic Ridge MORB	Volcanic tephra and impact outfall	
	• Volcanic arcs	Temperature rise	
	• Rift degassing	Increasing aridity	
	Major impacting		Atmosphric hazard
	Volcanic tephra and impact outfall	Transgressive System Tracks (TST) → Maximum Flooding Surfaces (MFS)	Acid sturz rain,
Negative	Plate motion		Flash flood
Ozone loss (0.25)	Solar radiation	Tidal dissipation	Mass flow, siliciclastics fining upward cycles (FUC)
Sulfate and smoke (0.55)	Milankovitch Cycles Moon recession rate Earth's rotational velocity	Black shale, Tuffite	Loss of mineral content → quartz arenite
Clouding increase (0.4)		pH, Eh-decreasing	Reworking, resedimentation
Tephra: Pinatubo up to −3.2 (8/1992)		Acidification Decreasing $\partial^{13}C$	Hydromorphic soil
			Kaolinite
		Volcanic tephra and impact outfall	
		Temperature fall	
		Increasing humidity	
		Cosmic winter, mass extinction	

Negative climate forcing directs MFSs, humid/warm conditions, pH < 7, acid rain, mass flow, growth of shelf areas (tidal dissiptation), toxic metals, loss of feldspar and unstable heavy metals → quartz arenite (K6.1 → K6.2).

Multiple impacting coincides with: a significant change of the Moon's recession rate and Earth's Mantle rotational energy, an over-regional unconformity and mass extinction at the Carnian/Norian boundary, onset of the "amalgamated" paleosol and the "amalgamated" MFSs Tr 70a,b,c on the Jordanian Platform], and a modification of the clay mineral assemblage in the Germanic Basin during maximum opening of the PAO. How important are tephras in the Upper Triassic pelites?

Through the Norian both "amalgamated" MFSs Tr 70a,b,c and TR 80a,b (**Figure 4B**) continued impacting (Manicouagan, Rochechouart, Obolon) (**Table 2**), recurrent "boundary clay suspicious claystone", and ongoing PAO rifting/degassing [7] dominated both study areas.

The TJB mass extinction meets LIP triggered degassing (NT, PAO, CAMP) and impacting (PDS in quartz grains).

Table 5 summarizes the interconnections and cause/effect patterns we recorded throughout our Triassic excursion.

7. Closing Statement

Geo-scientific interplaying appears as a revisit of playing in a golden childhoods' sandpit.

Acknowledgements

We are grateful to the authors who provided the data of driving processes for interpretation of the effects on sedimentary systems. Best thanks to Kjell Paris for digital support.

Conflicts of Interest

The authors declare no conflicts of interest regarding the publication of this paper.

References

[1] Schneider, W. and Salameh, E. (2012) Did Major Impacts Affect Sedimentologic/Sequence-Analytical Patterns of the Early Palaeozoic Sedimentary Systems of Jordan, Arabian Plate? *Open Journal of Geology*, **2**, 241-252. https://doi.org/10.4236/ojg.2012.24024

[2] Schneider, W. and Salameh, E. (2020) Phanerozoic Quartz Arenite Formation and Sequence Analytical Patterns: Indirectly Relating to Major Impacting and Super Plume Volcanism, Jordan, Arabian Plate. *Open Journal of Geology*, **10**, 13-52. https://doi.org/10.4236/ojg.2020.101002

[3] Price, N. (2001) Major Impacts and Plate Tectonics. Routledge, London, 354 p. https://doi.org/10.1201/9780203165454

[4] White, R.W. and Saunders, A.D. (2005) Volcanism, Impact and Mass Extinction:

Incredible or Credible Coincidences? *Lithos*, **79**, 299-316.
https://doi.org/10.1016/j.lithos.2004.09.016

[5] Peterson, S.V., Dutton, A. and Lohman, K.C. (2016) End-Cretaceous Extinction in Antarctica Linked to Both Deccan Volcanism and Meteoritic Impact via Climate Change. *Nature Communications*, **7**, Article No. 12079.
https://doi.org/10.1038/ncomms12079

[6] Henehan, M.J., Ridgwell, A., Thomas, E., Zhang, S., Alegret, L., Schmidt, J.R., Planavsky, N.J. and Hull, P.M. (2019) Rapid Ocean Acidification and Protracted Earth System Recovery Followed the End-Cretaceous Chicxulub Impact. *Proceedings of the National Academy of Sciences of the United States of America*, **116**, 22500-22504.
https://doi.org/10.1073/pnas.1905989116

[7] Dobretsov, N.L., Vernikovski, V.A., Karyakin, Y.V., Korago, E.A. and Simonov, V.A. (2013) The Mesozoic-Cenozoic Volcanism and Stages of the Geodynamic Evolution of the Central Eastern Arctic. *Russian Geology and Geophysics*, **54**, 1126-1144.
https://doi.org/10.1016/j.rgg.2013.07.008

[8] Svensen, H.H., Torsvik, T.H., Callegaro, S., Augland, L., Heimdal, T.H., Jerram, D.A., Planke, S. and Pereira, E. (2017) Gondwana Large Igneous Provinces: Plate Reconstructions, Volcanic Basins and Sill Volumes. In: Sensarma, S. and Storey, B. C., Eds., *Large Igneous Provinces from Gondwana and Adjacent Regions*, Vol. 463, Geological Society, London, 17-40. https://doi.org/10.1144/SP463.7

[9] Svensen, H.H., Jerram, D.A., Polozov, A.G., Planke, S., Neal, C.R., Augland, L.E. and Emeleus, H.C. (2019) Thinking about LIPs: A Brief History of Ideas in Large Igneous Province Research. *Tectonophysics*, **760**, 229-251.
https://doi.org/10.1016/j.tecto.2018.12.008

[10] Self, S., Schmidt, A. and Mather, T.A. (2014) Emplacement Characteristics, Time Scales, and Volcanic Gas Release Rates of Continental Flood Basalt Eruptions on Earth. In: Keller, G. and Kerr, A.C., Eds., *Volcanism, Impacts, and Mass Extinctions: Causes and Effects*, Vol. 505, Geological Society of America, Boulder, 319-337.
https://doi.org/10.1130/2014.2505(16)

[11] Augland, L.E., Ryabov, V.V., Vernikovsky, V.A., Planke, S., Polozov, A.G., Callegaro, S., *et al.* (2019) The Main Pulse of the Siberian Traps Expanded in Size and Composition. *Scientific Reports*, **9**, Article No. 18723.
https://doi.org/10.1038/s41598-019-54023-2

[12] Svensen, H., Planke, S., Polozov, A.G., Schmidbauer, N., Corfu, F., Podladchikov, Y.Y., *et al.* (2009) Siberian Gas Venting and the End-Permian Environmental Crisis. *Earth and Planetary Science Letters*, **277**, 490-500.
https://doi.org/10.1016/j.epsl.2008.11.015

[13] Schmincke, H.U. (2000) Vulkanismus. Wissenschaftliche Buchgesellschaft, Darmstadt, 264 p.

[14] Geyer, M., Nitsch, E. and Simon, T. (2011) Geologie von Baden-Württemberg [Geology of the State of Baden-Württemberg, Germany]. Schweizerbart Science Publishers, Stuttgart.

[15] German Stratigraphic Commission, Menning, M. and Hendrich, A. (2017) Stratigraphic Table of Germany Compact 2017. GFZ German Research Centre for Geosciences, Potsdam.

[16] DSK: Stratigraphie von Deutschland IV: Keuper (2005) Bearbeitet von der Arbeitsgruppe Keuper der Subkommission Perm-Trias der DSK Red.: Deutsche Stratigraphische Kommission(Hrsg.) Beutler, Gerhard (Koord. und Red.) Hauschke, N.; E. Nitsch; U. Vath [Stratigraphy of Germany IV: Keuper (upper Triassic)] 2005. 296

Seiten, 64 Abbildungen, 50 Tabellen, 2 Tafeln, 21x30cm, 1220 g

[17] Koch, G. and Schneider, W. (1985) Der Obere Keuper Südost-Niedersachsens in Übertage-Aufschlüssen—Fazies und Mineralbestand. *Bericht der Naturhistorischen Gesellschaft zu Hannover*, **128**, 19-48.

[18] Schneider, W. (2000-2015) Mapping Work in the Upper Triassic, Bl. Tübingen und Umgebung/SW Deutschland, 1:50.000. Landesamt für Geologie, Rohstoffe und Bergbau, Freiburg im Breisgau.

[19] Spray, J.G., Kelly, S.P. and Rowley, D.B. (1988) Evidence for a Late Triassic Multiple Impact Events on Earth. *Nature*, **392**, 171-173. https://doi.org/10.1038/32397

[20] Rampino, M.R. and Heggerty, B.M. (1994) Extraterrestrial Impacts and Mass Extinctions of Life. In: Gehrels, T.G., Ed., *Hazards Due to Comets & Asteroids*, University of Arizona Press, Tucson, 827-857. https://doi.org/10.2307/j.ctv23khmpv.33

[21] Hodych, J.P. and Dunning, G.R. (1992) Did the Manicouagan Impact Trigger End-Triassic Mass Extension? *Geology*, **20**, 51-54. https://doi.org/10.1130/0091-7613(1992)020<0051:DTMITE>2.3.CO;2

[22] Dunning, G.R. and Hodych, J.P. (1990) U/Pb Zircon and Baddelleyite Ages for the Palisades and Gettysberg Sills of the NE United States: Implications for the Age of the Triassic/Jurassic Boundary. *Geology*, **18**, 795-789. https://doi.org/10.1130/0091-7613(1990)018<0795:UPZABA>2.3.CO;2

[23] Bice, D.M., Newton, G.R., Mccauley, S., Reiners, P.W. and Mcroberts, C.A. (1992) Shocked Quartz at the Triassic/Jurassic Boundary in Italy. *Science*, **229**, 443-446. https://doi.org/10.1126/science.255.5043.443

[24] Sharland, P.R., Casey, D.M., Davies, R.B., Simmons, M.D. and Sut-Cliffe, O.E. (2004) Arabian Plate Sequence Stratigraphy—Revisions to SP2. *GeoArabia*, **9**, 199-214. https://doi.org/10.2113/geoarabia0901199

[25] Haq, B.U. and Al-Qahtani, A.M. (2005) Phanerozoic Cycles of Sea-Level Change on the Arabian Platform. *GeoArabia*, **10**, 127-160. https://doi.org/10.2113/geoarabia1002127

[26] Abdelmalak, M.M., *et al*. (2018) Break-Up Volcanism and Plate Tectonicscin the NW Atlantic. *Tectonophysics*, **760**, 229-251.

[27] Heimdal, T.H., Jones, M.T., Svensen, H.H., Callegaro, S. and August, M. (2020) LIP of the Month. The Central Atlantic Magmatic Province (CAMP) and the End-Triassic Crisis. Large Igneous Provinces Commission, Oslo, 1-12.

[28] Bullard, E., Everett, J.E. and Gilbert Smith, A. (1965) The Fit of the Continents around the Atlantic. *Philosophical Transactions of the Royal Society of London. Series A, Mathematical and Physical Sciences*, **258**, 41-51. https://doi.org/10.1098/rsta.1965.0020

[29] Schneider, W. and Salameh E. (2022) The Permian-Triassic Transitional Zone: Jordan, Arabian Plate; Linked to Siberian Large Igneous Province and Neo-Tethys Breakup Degassing via Climate Forcing, Atmospheric Hazard and Metal Toxicity. *Open Journal of Geology*, **12**, 472-503. https://doi.org/10.4236/ojg.2022.126023

[30] Schneider, W. and Salameh, E. (2020) End-Cretaceous Quartz Arenite Formation in an Estuarian Environment under Brine Influence, N. Germany; Linked to both Deccan Volcanism and Chicxulub Impact Degassing during Climate Change. *Open Journal of Geology*, **10**, 1091-1118. https://doi.org/10.4236/ojg.2020.1011053

[31] Bandel, K. and Khoury, H. (1981) Lithostratigraphy of the Triassic in Jordan. *Facies*, **4**, 1-26. https://doi.org/10.1007/BF02536584

[32] Amireh, B.S. (1987) Sedimentological and Petrological Interplays of the Nubian Se-

ries in Jordan with Regard to Paleogeography and Diagenesis. Technische Universität Carolo Wilhelmina, Braunschweig, 232 p.

[33] Powell, J.H., Stephenson, M.H., Nicora, A., Rettori, R., Borlenghi, L.M. and Cristina Perri, M.C. (2016) The Permian-Triassic Boundary, Dead Sea, Jordan: Transitional Alluvial to Marine Depositional Sequences and Biostratigraphy. *Rivista Italiana di Paleontologia e Stratigrafia*, **122**, 23-40

[34] Amireh, B.S. (1993) Three Paleosols of the Nubian Series of Jordan: Climatologic, Tectonic and Paleogeographic Implications. *Dirasat*, **20B**, 33-62.

[35] Jarrar, G. (1991) Petrology and Geochemistry of a Triassic Subvolcanic Suite from Central Jordan, East and Northeast of the Dead Sea. *Mu'tah Journal for Research and Studies*, **6**, 183-196.

[36] Dvorkin, A. and Kohn, B.P. (1989) The Asher Volcanics, Northern Israel: Petrography, Mineralogy, and Alteration. *Israel Journal of Earth Sciences*, **38**, 105-123.

[37] Beutler, G. (1998) Keuper. *Hallé'sches Jahrbuch Geowissenschaften*, *Reihe B*, *Beihefte*, **5**, 45-58.

[38] Walter, R. (2007) Geologie von Mitteleuropa. 7th Edition, Schweizerbart Science Publishers, Stuttgart, 511 p.

[39] Miall, D. (1996) The Geology of Fluvial Deposits, Sedimentary Facies, Basin Analysis, and Petroleum Geology. Springer, Berlin, 582 p.

[40] Schneider, W. (1973) Zur Genese der Gipskeuper-Dolomitee am Suedrand der Luxemburger Ardennen. *Oberrheinische Geologische Abhandlungen*, **22**, 51-74.

[41] Kern, A. and Aigner, T. (1997) Faziesmodell für den Kieselsandstein (Keuper, Obere Trias) von SW-Deutschland: Eine terminale alluviale Ebene. *Neues Jahrbuch für Geologie und Paläontologie-Monatshefte*, No. 5, 267-285. https://doi.org/10.1127/njgpm/1997/1997/267

[42] Kulke, H. (1969) Petrographie und Diagenese des Stubensandsteines (mittlerer Keuper) aus Tiefbohrungen im Raum Memmingen (Bayern). *Contributions to Mineralogy and Petrology*, **20**, 135-163. https://doi.org/10.1007/BF00399628

[43] Engelhardt, W. (1973) Die Bildung von Sedimenten und Sedimentgesteinen. In: *Sediment-Petrograohie*, Teil III, Schweizerbart Science Publishers, Stuttgart, 378 p.

[44] Lippmann, F. and Zimmerman, M. (1983) Die Petrographie des Knollenmergels, Mittlerer Keuper, Trias. *Geologische Rundschau*, **72**, 1105-1153. https://doi.org/10.1007/BF01848356

[45] Appel, D. (1981) Petrographie und Genese der Sandsteine des Unter-und Mittelrhät in Nördlichen Harzvorland (Ostniedersachsen). Leibniz Universität Hannover, Hannover, 133.

[46] Koch, G. and Schneider, W. (1985) Der Obere Keuper SE-Niedersachsen in Übertage Aufschlüssen—Fazies und Mineralbestand. *Bericht der Naturhistorischen Gesellschaft zu Hannover*, **128**, 19-48.

[47] Hauschke, K.,und Wilde, V. (1996) Fazies und Fossilfuhrung in Unterrhät des Fuchsberges bei Seinstedt (nördliches Harzvorland, Niedersachsen). *Hallé'sches Jahrbuch für Geowissenschaften Halle*, **18**, 151-152.

[48] Will, H.-J. (1969) Untersuchungen zur Strategraphie und Genese des Oberkeupers in NW Duetschland. *Geologisches Jahrbuch*, *Beihefte*, **54**, 240 p.

[49] Aigner, T. and Bachman G.H. (1992) Sequence-Stratigraphic Framework of the German Triassic. *Sedimentary Geology*, **80**, 115-135. https://doi.org/10.1016/0037-0738(92)90035-P

[50] Aigner, T. and Bachman, G.H. (1998) Sequence-Stratigraphy of the German Trias-

sic. A Short Overview. *Halle'isches Jahrbuch fur Geowissenschaften. Reihe B*, **6**, 23-26.

[51] Stow, D.A.V. (1986) Deep Clastic Seas. In: Reading, H.S., Ed., *Sedimentary Environments and Facies*, 2nd Edition, Blackwell, Oxford, 399-444.

[52] Uhl, D., Abu Hamad, A., Kerp, H. and Bandel, K. (2007) Evidence for Palaeo-Wildfire in the Permian Palaeotropics—Charcoalified Wood from the Um Irna Formation of Jordan. *Review of Palaeobotany and Palynology*, **144**, 221-230. https://doi.org/10.1016/j.revpalbo.2006.08.003

[53] Lippman, F. (1954) Über einen Keuperton von Zaisserweiser bei Maulbronn. Heidelberger Beitr. *Heidelberger Beiträge zur Mineralogie und Petrographie*, **4**, 130-134. https://doi.org/10.1007/BF01111150

[54] Lippman, F. (1960) Corrensit. In: Hintze, C., Ed., *Handbuch der Mineralogie*, De Gruyter, Berlin, 668-691.

[55] Heerde, W. (1979) Tonmineral. Untersuchungen an Sedimenten des Mittleren und Oberen Keupers, des Untern Jura und des Tertiärs B1, Süpplingen (3731), N. Germany, Dipl. Arb. Braunschweig Technical University, Braunschweig, 150.

[56] Tanner, L.H. (2010) The Triassic Isotopes. In: Lucas, S.G, Ed., *The Triassic Timescale*, Vol. 334, Geological Society, London, Special Publications, 103-108. https://doi.org/10.1144/SP334.5

[57] Creer, K.M. (1975) On the Tentative Correlation between Changes in the Geomagnetic Polarity Bias and Reversals Frequency and the Earth's Rotation through Phanerozoic Time. In: Rosenberg, G.D. and Runcorn, S.K., Eds., *Growth Rhythms and the History of the Earth's Rotation*, Wiley, London, 293-318.

[58] Garland, G.D. (1971) Introduction to Geophysics: Mantle, Core and Crust. Saunders, Philadelphia, 420 p.

[59] van Andel, T.H. (1994) New Views on an Old Planet. Cambridge University Press, Cambridge, 402. https://doi.org/10.1017/CBO9781139174114

[60] Panella, G. (1972) Paleontological Evidence on the Earth's Rotation History since Precambrian. *Astrophysics and Space Science*, **16**, 212-237. https://doi.org/10.1007/BF00642735

[61] Brink, H.-J. (2006) Do the Global Geodynamic Cycles of the Phanerozoic Represent a Feedback System of the Earth and is the Moon Involved as an Acting External Force? *Zeitschrift der Deutschen Gesellschaft für Geowissenschaften*, **157**, 17-40. https://doi.org/10.1127/1860-1804/2006/0157-0017

[62] Benton, M. (1986) More than One Event in the Late Triassic Mass Extinction. *Nature*, **321**, 857-861. https://doi.org/10.1038/321857a0

[63] Benton, M. (1987) Aktuelle Probleme der Evolutions-Forschung aus der Sicht Palaeontologen. In: Ditfurth, H.V., Ed., *Mannheimer Forum* 87/88, Boeringer Mannhein, Mannheim, 105-1166.

[64] Li, M., *et al.* (2016) Astronomical Tuning of the End-Permian Extinction and the Early Triassic Epoch of South China and Germany. *Earth and Planetary Science Letters*, **441**, 10-25. https://doi.org/10.1016/j.epsl.2016.02.017

[65] Milliman, J.D. (1974) Marine Carbonates. Recent Sedimentary Carbonates Part 1. Marine Carbonates. Springer-Verlag, Berlin, 375 p.

[66] Oppenheimer, C.H. and Master I.M. (1964) Transition of Silicates and Carbonate Crystal Structure by Photo Synthesis and Metabolism (Abstract). Geological Society of America, Special Paper 76, 125.

[67] Fritz, F. and Smith, D.G.W. (1970) The Isotopic Concentration of Secondary Dolomites. *Geochimica et Cosmochimica Acta*, **34**, 1161-1173.

https://doi.org/10.1016/0016-7037(70)90056-6

[68] Behrends, E.W. and Land, L.S. (1972) Subtidal Holocene Dolomite, Baffin Bay, Texas. *Journal of Sedimentary Petrology*, **42**, 155-161.

[69] Millot, G. (1970) Geology of Clays: Weathering, Sedimentology, Geochemistry. Springer, Berlin, 425 p. https://doi.org/10.1007/978-3-662-41609-9

[70] Hsü, K.J. (1988) Cretaceous/Tertiary boundary sediment. In: Edward Clifton, H., Ed., *Sedimentologic Consequences of Convulsive Geologic Events*, Geological Society of America, Boulder. https://doi.org/10.1130/SPE229-p143

[71] Tschudy, R.H., Pillmore, C.L., Orth, C.J., Gilmore, J.S. and Knight, J.D. (1884) Disruption of the Terrestrial Planet Ecosystem at the Cretaceous/Tertiary Boundary. *Science*, **225**, 1030-1032. https://doi.org/10.1126/science.225.4666.1030

[72] Orth, C.J., et.al. (1982) Irdium Abundance Measurements across the Cretaceous/Tertiary Boundary in the San Juan and Raton Basins of Northern New Mexico. In: Silver, L.T. and Schultz, P.H., Eds., *Geological Implications of Impacts of Large Asteroids and Comets on the Earth*, Geological Society of America, Boulder, 423-434. https://doi.org/10.1130/SPE190-p423

[73] Bohor, B.F., Foord, E.E., Modreski, P.J., Triplehorn, D.M. and Mineralogic, S. (1984) Mineralogic Evidence for an Impact Event at the Cretaceous-Tertiary Boundary. *Science*, **224**, 867-869. https://doi.org/10.1126/science.224.4651.867

[74] Pillmore, C.L., Tschudyc, R.H., Orthj, J., Gilmore, S. and Knight, J.D. (1984) Geologic Framework of Nonmarine Cretaceous-Tertiary Boundary Sites, Raton Basin, New Mexico and Colorado. *Science*, 223, 1180-1183. https://doi.org/10.1126/science.223.4641.1180

[75] Smit, J. and Romein, A.J.T. (1985) A Sequence of Events across the Cretaceous-Tertiary Boundary. *Earth and Planetary Science Letters*, **74**, 153-170. https://doi.org/10.1016/0012-821X(85)90019-6

[76] Pierazzo, E., Kring, D.A. and Melosh, H.J. (1998) Hydrocode Simulation of the Chicxulub Impact Event and the Production of Climatically Active Gases. *Journal of Geophysical Research*: *Planets*, **103**, 28607-28625. https://doi.org/10.1029/98JE02496

[77] Stöffler, D. (2002) Bedrohung aus dem Weltall—Asteroiden und Kometen. In: Emmermann, R., Balling, R., Hasinger, G., Heiker, F.R., Schütt, C., Walther, D. and Donner, W., Eds., *An den Fronten der Forschung*: *Kosmos-Erde-Leben*, S. Hirzel Verlag, Stuttgart, 81-98.

[78] Krauskopf, K.B. (1982) Introduction to Geochemistry. McGraw-Hill International, London, 617 p.

[79] Stähle, V., Frenzel, G., Hess, J.C. Saupe, F., Schmidt, S.T. and Schneider, W. (2001) Permian Metabasalt and Triassic Alkaline dykes in the Northern Ivrea Zone: Clues to the post-Variscan Geodynamic Evolution of the Southern Alps. *Schweizerische Mineralogische und Petrographische Mitteilungen*, **81**, 1-21.

[80] Sanders, C.A.E., Bertotti, G., Tomassini, S., Davies, G.R. and Wijbrans, J.S. (1996) Triassic Pegmatite in the Mesozoic Middle Crust of the Southern Alps (Italy): Fluid Inclusions, Radiometric Dating and Tectonic Implications. *Eclogae Geologicae Helvetiae*, **89**, 505-525.

[81] Nic, S.D.K. and Yang, C.S. (1991) Sea-Level Fluctuation and the Geometric Variability of the Tide-Dominant Sandbodies. *Sedimentary Geology*, **70**, 161-193. https://doi.org/10.1016/0037-0738(91)90140-9

[82] Schneider, W., Amireh, B.S. and Abed, A.M (2007) Sequence Analysis of the Early

Paleozoic Sedimentary Systems of Jordan. *Zeitschrift der Deutschen Gesellschaft für Geowissenschaften*, **158**, 225-247.
https://doi.org/10.1127/1860-1804/2007/0158-0225

Appendix

Architectural elements and lithofacies types in fluvial- and tide-dominated sand bodies [39] [81] [82]

Architectural elements in fluvial deposits and from tidal sand bodies:

CH	Channel	Any combination	
GB	Gravel bars and bedforms	Gm, Gp, Gt	
SB	Sandy bedforms	St, Sp, Sh, Sl, Sr, Se, Ss	
SG	Sediment gravity flow	Sm, Sh	C Carbonaceous mud
DA	Downstream accretion	St, Sp, Sh, Sl, Sr, Se, Ss	
LA	Lateral accretion macroform	St, Sp, Sh, Sl, Se, Ss minor Gm, Gp	
LS	Laminated sand sheet	Sh, Sl, minor Sp, Sr	P paleosol
FF	Overbank fine sediments	Fl, Fm	
MF	Mixed tidal flats	St, Sw, St, Fr, Fl	
SF	Sandy tidal flats	St, Sp, Sw, Sl, Sr	
SW	Sand waves	St, Sp, Sh, Sl, Sr	
TB	Tidal bar	St, Sr, Fr, Ss, Sf, Sw	
T	Tempestite	Sh, Fl, Hes, Scs, Sw	
TCH	Tidal to subtidal channel	Sm, St, Sp, Sh	

Fluvial and tidal/marine lithofacies types:

Facies code	Lithofacies	Sedimentary structures
Gmm	Matrix-supported, massive gravel	Weak grading
Gcm	Clast-supported massive gravel	Pseudoplastic debris flow
Gt	Gravel, stratified	Trough cross-beds
Gp	Gravel, stratified	Planar cross-beds
St	Sand, medium to very coarse, may be pebbly	Solitary or grouped trough cross-beds
Sp	Sand, medium to very coarse, may be pebbly	Solitary or grouped planar cross-beds
Sr	Sand, very fine to coarse	Ripple marks of all types
Sh	Sand, very fine to very coarse, may be pebbly	Horizontal lamination, parting lineation
Sm	Sand, fine to coarse	Massive or faint lamination
Ss	Sand, very fine to coarse, may be pebbly	Broad, shallow scours
Sl	Sand, very fine to coarse, may be pebbly	Low angle ($<15^0$) cross-beds
Spo	Sand, fine to coarse	Overturned planar cross-beds
Sto	Sand, fine to coarse	Overturned trough cross-beds
Sf	Fine sand with mud	Flaser-rippled stratification
Sw	Fine sand with mud	Wave-rippled stratification
Hca	Fine sand with mud	Hummocky cross0stratification
Scs	Fine sand with mud	Swaley cross-stratification
Fr	Sand, silt, mud	Ripple to climbing ripple cross-lamination
Fm	Sand, silt, mud	Massive
Fl	Sand, silt, mud	Fine lamination, very small ripples